

Thermodynamic evaluation of bi-directional solid oxide cell systems including year-round cumulative exergy analysis

Botta, G.; Mor, R.; Patel, H.; Aravind, P. V.

DOI

[10.1016/j.apenergy.2018.05.061](https://doi.org/10.1016/j.apenergy.2018.05.061)

Publication date

2018

Document Version

Final published version

Published in

Applied Energy

Citation (APA)

Botta, G., Mor, R., Patel, H., & Aravind, P. V. (2018). Thermodynamic evaluation of bi-directional solid oxide cell systems including year-round cumulative exergy analysis. *Applied Energy*, 226, 1100-1118. <https://doi.org/10.1016/j.apenergy.2018.05.061>

Important note

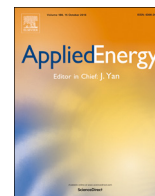
To cite this publication, please use the final published version (if applicable). Please check the document version above.

Copyright

Other than for strictly personal use, it is not permitted to download, forward or distribute the text or part of it, without the consent of the author(s) and/or copyright holder(s), unless the work is under an open content license such as Creative Commons.

Takedown policy

Please contact us and provide details if you believe this document breaches copyrights. We will remove access to the work immediately and investigate your claim.



Thermodynamic evaluation of bi-directional solid oxide cell systems including year-round cumulative exergy analysis



G. Botta*, R. Mor, H. Patel, P.V. Aravind

Process & Energy Department, Delft University of Technology, Leeghwaterstraat 39, 2628CB Delft, Netherlands

HIGHLIGHTS

- CE method can be used next to round trip efficiency to design Bi-SOC systems.
- Bi-SOC year-round cumulative exergy efficiency varies from 33% to 73%.
- Bi-SOC energy efficiencies range between 29% and 66%.
- Bi-SOC performance is higher for different operating condition of SOFC and SOEC.

ARTICLE INFO

Keywords:

Bi-directional solid oxide cells
Energy storage
Power production
Power-to-gas
Renewable energy
Year-round cumulative exergy analysis

ABSTRACT

Bi-directional solid oxide cell systems (Bi-SOC) are being increasingly considered as an electrical energy storage method and consequently as a means to boost the penetration of renewable energy (RE) and to improve the grid flexibility by power-to-gas electrochemical conversion. A major advantage of these systems is that the same SOC stack operates as both energy storage device (SOEC) and energy producing device (SOFC), based on the energy demand and production. SOEC and SOFC systems are now well-optimised as individual systems; this work studies the effect of using the bi-directionality of the SOC at a system level.

Since the system performance is highly dependent on the cell-stack operating conditions, this study improves the stack parameters for both operation modes. Moreover, the year-round cumulative exergy method (CE) is introduced in the solid oxide cell (SOC) context for estimating the system exergy efficiencies. This method is an attempt to obtain more insightful exergy assessments since it takes into account the operational hours of the SOC system in both modes. The CE method therefore helps to predict more accurately the most efficient configuration and operating parameters based on the power production and consumption curves in a year.

Variation of operating conditions, configurations and SOC parameters show a variation of Bi-SOC system year-round cumulative exergy efficiency from **33% to 73%**. The obtained thermodynamic performance shows that the Bi-SOC when feasible can prove to be a highly efficient flexible power plant, as well as an energy storage system.

1. Introduction

Efficient electrical energy storage and power-to-gas solutions could play a substantial role in increasing the penetration of fluctuating renewable energy resources, thus mitigating the worst impacts of climate change, and in integrating different energy grids and infrastructures [1–8]. Among the various technologies, solid oxide electrolyser cell (SOEC) is currently the focus of numerous research and development efforts because it converts electricity into chemical energy with a higher efficiency compared to alkaline electrolyser and proton exchange membrane electrolyser technologies [9]. Moreover, to the present

knowledge, SOECs are the only electrolyser cells that have shown the possibility of operating in reversible mode without exhibiting severe degradation [10,11]. This allows them to compete with compressed air and pumped hydro energy storage methods, and advanced batteries [12–14].

Bi-directional solid oxide cell (Bi-SOC) systems store electricity by producing a synthetic fuel in the electrolysis mode and generating electricity by electrochemically oxidising fuel in fuel cell mode, based on the energy demand and production [12–14]. Fig. 1 sketches the working principle of a Bi-SOC system where power is produced from biomass-derived syngas or from H₂, and can then be used for a wide

* Corresponding author.

E-mail address: g.botta@tudelft.nl (G. Botta).

Nomenclature*Symbols*

A	cell/stack area [m ²]
\dot{E}	molar energy flow rate of the fuel on the basis of LHV [kW]
Ex	exergy [kW]
F	Faraday constant [C/mol]
h	molar enthalpy of component [kJ/mol]
I	current [A]
J	current density [A/m ²]
\dot{n}	mole flow rate [kmol/s]
P	pressure [bar]
\dot{Q}	heat flow rate [kW]
T	operating temperature [°C]
t	operational hours [hours]
V	voltage [V]
\dot{W}	work flow rate [kW/MW]
z	number of electrons generated/required per electro-chemical reaction [–]
η	efficiency [%]

Subscripts

D	destruction
---	-------------

ec	electrolyser cell
fc	fuel cell
in	inlet
k	component k
NST	nernst
out	outlet
sys	system

Abbreviations

ASR	area specific resistance
Bi-SOC	bi-directional SOC
CE	cumulative exergy
GT	gas turbine
LHV	lower heating value
REaccuracy	relative error
ReSOC	reversible SOC
SOC	solid oxide cell
SOFC	solid oxide fuel cell
SOEC	solid oxide electrolyser cell
UF	utilisation factor
TIT	turbine inlet temperature

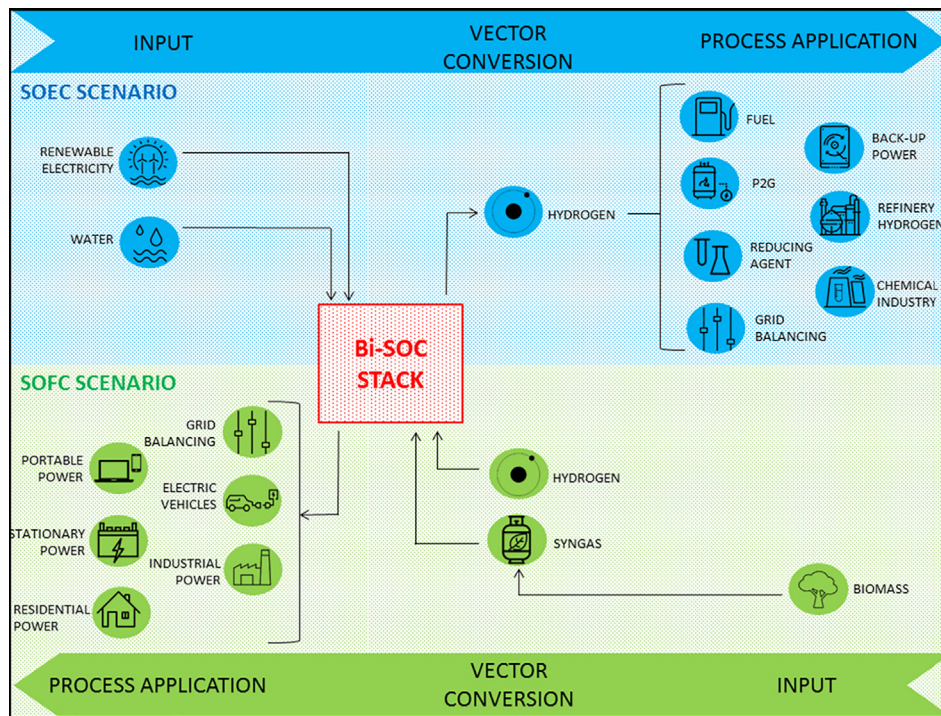


Fig. 1. Bi-SOC energy system.

array of applications. Analogously, H₂ is produced from H₂O in the electrolysis mode, using a renewable energy source (e.g., solar, wind, hydro). The H₂ produced can then be used in other processes, converted to others chemicals, or can be stored and converted again to power by the same Bi-SOC operating in the fuel cell mode when necessary.

Potentially, Bi-SOC systems are flexible regarding both the fuel and the energy sources fed to, compatible with reduced CO₂ emission targets in power generation mode, adaptable to local energy needs and to different applications [10]. However, this is not yet a sufficiently

mature technology to set up efficient and cost-effective operation. Moreover, SOCs are now optimised for one mode only, while Bi-SOCs must operate efficiently in both SOFC and SOEC modes.

SOFC systems have been extensively investigated. Recent works focused on the optimization of SOFC and combined SOFC-Gas Turbine (SOFC-GT) systems. A techno-economic optimization of a SOFC micro-combined heat and power (CHP) systems (10–20 kW size range) is presented by Braun [15]. The system configurations and operating parameter selections could allow a minimum life-cycle cost while

achieving maximum CHP-system efficiency, reaching a life-cycle cost abatement of over 30% and CHP efficiency improvements of about 20% as compared to the base scenarios. Whiston et al. introduced an exergetic and economic comparison between the performance of a SOFC-GT system and of a SOFC system [16]. Even if combined systems are still in the demonstration phase, the study upholds hybrid systems's continued investigation and development since the hybrid system generated power more efficiently (66% exergy efficiency) than the stand-alone SOFC system (59% exergy efficiency). Via a parametric study, Khani et al. [17] carried out an energy and exergo-economic evaluation of a SOFC-GT-absorption chiller system, studying the influences of key operating parameters on the performance of the system. A series of optimal working conditions are proposed and combining the SOFC with a gas turbine resulted in a higher exergy efficiency (+6.5%). The stack was the highest contributor to the total irreversibility. Bang-Møller et al. [18] performed an exergy analysis and optimization of a hybrid plant consisting of a two-stage gasifier, SOFC and GT resulting in a gain of 6% in electrical efficiency when integrating the heat management. The optimal configuration produced 290 kWe reaching an electrical efficiency of 58% based on LHV. A cogeneration plant containing an SOFC, a GT, an air preheater, and an inlet air cooling system was optimized by Hajabdollahi et al. [19], considering the presence of combustion chambers, heat exchangers, inlet air cooling system and SOFC as design variables. The system containing the SOFC resulted in lower exergy destruction in the air compressor and higher exergy destruction in the heat recovery steam generator. Hosseinpour et al. presented, and optimized from energy and exergy perspectives, a cogeneration system consisting of SOFC and a Stirling engine [20]. The energy efficiency of the combined system was about 76%, while that of the stand-alone SOFC plant was around 25% lower. The combined system reached a maximum exergy efficiency of about 56%, and in both systems the air heat exchanger had the greatest exergy destruction rate.

When compared to SOFC or other electrolyzers, SOEC is still young and relatively unexplored. However, there have been rapid and interesting developments in SOECs, displaying that this technology is up-and-coming in a near future [21–23]. Unfortunately, costs are still high [24]. Techno-economic analyses and system design have been performed mainly in recent years. De Saint Jean et al. carried out an economic assessment of a power to methane system via SOEC and CO₂ methanation [25]. The resulting high cost of SNG were associated with the cost of SOEC stacks and their performance degradation. Varone et al. presented an economic evaluation of 50 MWe power-to-liquid plant producing methanol from renewable energy via SOECs [26]. The estimated cost of renewable methanol production was competitive with the present production methods. Guendalini et al. showed that acceptable conditions for efficient and economic viable power-to-gas for improved wind energy dispatchability are possible and they might be further improved with a reduction of the electrolyser cost and electricity price [27]. A SOEC model developed in Aspen Plus™ is presented and used in [28] to execute a parametric analysis, and an energy and exergy assessment. The highest energy and exergetic efficiency resulted in about 78% and 92%, respectively. Sunfire GmbH in the last few years has been involved in several projects where high temperature electrolysis was integrated in power-to-gas or power-to-liquid technologies [29–33]. Also Haldor Topsoe, during recent years, started intensively researching SOEC for power-to-gas, mostly from a theoretical and system design perspective [34–37]. Moritz et al. have shown that increasing pressure (from 0.05 to 2 MPa) improved kinetics and mass transport in SOEC, but influenced negatively its thermodynamic efficiencies. When working at low pressure, the SOEC resulted in higher performance if operating at lower current densities. Conversely, at higher pressure the SOEC was more efficient if operating at higher current densities [38].

While SOFC has been largely investigated and SOEC is being recently studied, only a limited number of studies has been directed on Bi-SOC technology. Sunfire GmbH carried out a stack test with 26 cycles

switching between SOFC and SOEC mode at low current densities (0.3–0.4 A/cm²). The stack presented a 0.06% degradation per ReSOC cycle [39]. Graves et al. have shown that serious electrolysis-induced degradation can be erased by cycling between electrolysis and fuel-cell modes [11]. Perna et al. used a thermo-electrochemical model built in Aspen Plus™ to analyse a ReSOC unit fed with syngas and H₂ [40]. A round trip efficiency of about 70% was obtained when the system ran under its optimal conditions at low temperature (700 °C). A thermodynamic approach was used to investigate the influence of key operating parameters on the performance of a ReSOC by Wendel et al. [41]. While pressurized systems achieved high efficiency at high temperature and fuel utilisation, non-pressurized systems required lower temperature and energy density. Kazempour et al. developed and validated a model to analyse the performance of reversible operation SOC under several operating conditions [42]. The results showed that the total electrochemical losses of the cell can be very diverse between the two operative modes. A thermodynamic assessment of a ReSOC via a model developed using Aspen Plus™ is presented also by Hauck et al. [43], where it is pointed out that high temperature and high pressure could improve the performance of the ReSOC system, despite the still existing challenge of degradation, cost and transient operation. Mottaghizadeh et al. presented a process system model implemented with Aspen Plus™ [44]. A round trip efficiency of about 54% was obtained when working at ambient pressure, increasing to 60% when operating at 25 bar.

The scientific literature review clearly indicates that the cell-stack operating parameters have a great effect on system performance and optimizing the operating conditions to suit both modes is crucial to attain high Bi-SOC efficiency. However, Bi-SOC can hardly operate at maximum efficiency in both the modes when operated at the same conditions, thus having an impact on operating cost. For instance, reducing current density can improve performance in SOFC mode, but SOEC performance in terms of hydrogen production is lowered. Furthermore, while in SOFC mode voltage and over potential reduce with increasing temperature, resulting in better performance, higher exergy efficiency can be achieved in SOEC mode at low temperatures. Also, while high pressures increase the operating voltage and reduce diffusion losses thus boosting performance in SOFC mode, it is not clear if this is beneficial in SOEC mode since an increase in the Nernst potential is disadvantageous when working in electrolysis mode. Nonetheless, pressurizing the SOEC can be favourable at the system level. In fact, other aspects like water pressurization or hydrogen compression for storage, might justify the operation of SOEC systems at elevated pressure.

Only few system design studies aiming at optimising the stack parameters to work in both operating modes are currently available. Moreover, the commonly adopted exergy analysis method that is, round-trip efficiency, is insufficient in providing a practical estimation for such systems. In fact, despite being widely used, round trip efficiency analysis does not take into account the operating time in each mode and therefore cannot be probably used as sole criteria to design a bi-directional system.

This report presents the results from a steady state energy and exergy analyses for different bi-directional system configurations characterized by steam electrolysis when the stack operates in SOEC mode, and both syngas and H₂ oxidation when the stack operates in SOFC mode. We evaluated the effect of operating conditions, such as pressure, temperature, fuel utilisation, and current density, on the Bi-SOC system performance to address differences and similarities between SOC configurations for hydrogen and syngas oxidation and steam electrolysis. Furthermore, this paper introduces the application of the year-round Cumulative Exergy (CE) method into SOC context, a method proposed and used in literature to optimise energy systems considering their yearly based usage [45,46]. This method can be an extremely useful tool for identifying the components contributing the most to the exergy destruction and exhaust exergy losses based on the excess energy production and energy demand profile for a year. Therefore, the method

allows the identification of operating conditions and system configurations necessary to obtain high conversion efficiencies.

Section 2 of this paper describes the modelling approach and the calculation procedure used to quantitatively estimate energy and exergy flows of the SOC systems, and details the initial assumptions. The results section for the individual modes, Section 3, presents a series of SOC system configurations, from a simple system with minimal balance-of-plant (BoP) components to more complex systems including turbine-bottoming cycle. This section explores the sensitivity of the system performance to SOC stack parameters, thus seeking to optimise the process flow. Section 4 illustrates the results of the analysis carried out on the bi-directional systems. Sections 3 and 4 use the calculation method presented in Section 2 to draw the conclusions on the system energy and exergy performance. The paper concludes summarising the findings to appraise future Bi-SOC system design and analysis, providing a starting point for future research and proving the usefulness of the year-round CE method in selecting the favourable configuration and operating parameters.

2. Calculation methodology and modelling approach

This section introduces the hypotheses used in modelling the Bi-SOC stack and the system components, the methodology to calculate the Bi-SOC system performances metric definitions, the assumptions and the system operating conditions selected for the analysis.

2.1. SOC stack and system models

The first part of the subsection presents the mathematical modelling of the zero-dimensional SOC stacks, the electrochemical equations that characterize the stack and the main assumptions. The second part illustrates the system configuration and the BoP components modelling.

2.1.1. SOC stack modelling description and internal equations

Fuel cell and electrolyser are modelled in Aspen Plus™ using the available reactors, as well documented in literature [28,40,43,44,47]. Gibbs reactors are used to perform calculations based on the input reactant composition, temperature and pressure on the basis of Gibbs energy minimisation, whereas stoichiometric reactors are used to simulate the electrochemical reactions at specified operating conditions, and separators which reproduce the separation of the anode and cathode outcome flows, and they represent the electrolyte. The electrical and the heat required or produced are calculated via a mathematical model, which is coded in a calculator block using FORTRAN language. Our SOC components models, already presented in our previous work [48], have been built and validated through experimental results from DTU [49,50], as presented in Section 2.1.1.1.

In the literature, a wide range of SOFC or SOEC models are based on Faraday's current determined through an assumed utilisation factor [51–54]. The current, I , can be related to the total inlet molar flow of fuel (SOFC mode) or steam (SOEC mode), their respective utilisation factor and Faraday's relationship, Eqs. (1) and (2).

$$I_{fc} = zF\dot{n}_{fuel,in}UF_{fc} \quad (1)$$

$$I_{ec} = zF\dot{n}_{H_2O,in}UF_{ec} \quad (2)$$

Once the current is fixed, the lumped current density, J , can be obtained using the total active area of the SOC stack, for both SOFC and SOEC.

$$J = I/A \quad (3)$$

Commonly, SOFC or SOEC models are based on a linear approach [9,47,51,54]. The equations of the stack (4) and (5) represent the operative voltage of SOFC and SOEC stack as a function of the inlet Nernst potential [48] and an equivalent area specific resistance (ASR).

$$V_{fc} = V_{NST,in} - JASR \quad (4)$$

$$V_{ec} = V_{NST,in} + JASR \quad (5)$$

The ASR is calculated via an empirical expression, determined in Politecnico di Torino and presented by Giglio et al. in [55], Eq. (6).

$$ASR = 35.71 \exp[-0.0057(T_{in} - 273.15) - 0.0217P_{in}] \quad (6)$$

This equation is derived from the interpolation of experimental data from DTU [49,50], and it is valid in a range of 750–850 °C, and for pressure up to 10 bar [55].

The same ASR in both SOEC and SOFC modes is assumed in line with the work of Desideri et al. [56] and of Ferrero et al. [57].

The electrical power produced by the SOFC or demanded by the SOEC can be expressed as the product of the operative voltage (V_{fc}, V_{ec}) and the current, and it is related to the heat flow (\dot{Q}) through the energy balance. A modelling strategy to compute extra cooling/heating air is suggested by De Groot [53]. The SOC is enclosed within an adiabatic control volume, although the reaction is assumed to be at isothermal conditions. Then, assuming a constant temperature difference over the cell-stack, the necessary air flow can be determined through heat balance. Assuming inlet temperature equal to the reaction temperature, this heat balance can be written as in Eq. (7). Here, product molar flows see an enthalpy increase up to $h(P_{in}, T_{in})$, caused by the reaction heat \dot{Q}_{max} .

$$\sum [\dot{n}_{k,out} h_k(P_{in}, T_{out}) - \dot{n}_{k,in} h_k(P_{in}, T_{in})] = \dot{Q}_{max} \quad (7)$$

Therefore, in order to operate in highly endothermic or exothermic regions, extra air could be provided to heat up or cool down the cell [58,59]. However, temperature difference between SOEC outlet and inlet varies with the voltage, depending on its difference with thermoneutrality and it depends on the specific operating region. Therefore, the operating region is assumed in advance, as done by Fu et al. [58]. Constant temperature difference between the outlet and the inlet temperatures is 100 K when operating the stack as SOFC, and –100 K when operating the stack as endothermic SOEC.

Combining the equation to calculate the operative voltage, the global current density definition, and Faraday's law, the internal set of equations to be added to the conservation equations are obtained. Furthermore, Peng-Robinson equation has been selected as equation of state (EOS), since it is appropriate for rich hydrogen applications [47].

SOFC and SOEC assumptions summary [48]:

- Adiabatic SOC
- Constant utilisation factor
- Isothermal electrochemical reaction at SOC inlet temperature ($T_{iso} = T_{in}$)
- Isobaric electrochemical reaction at SOC inlet pressure ($P_{isob} = P_{in}$)
- Constant temperature difference between outlet and inlet temperatures, SOFC: $\Delta T = 100$ K and SOEC: $\Delta T = -100$ K
- Linear equation with $V_{NST,in}$ as reference voltage, and ASR based on operating temperature and pressure
- Same ASR assumed for both SOFC and SOEC modes

2.1.1.1. SOC model validation. The developed 0D isothermal models rely on the empirical ASR equation from Giglio et al. [55] and on lumped Nernst voltage calculated using the inlet compositions. The scope of this section is to provide the model validation through comparing the results predicted from our model and the results obtained in DTU [49,50]. In these publications the authors report experimental results of polarization curves in fuel cell and electrolyser modes at different pressures and compositions. Moreover, they also present overall ASR values. These can also be compared to the ASR values obtained through the slope of the IV curves from our model.

For the purpose of the validation, the fuel cell and electrolyser cell models are analysed without considering any extra elements in the flowsheet. In a SOC stack, several repeating cells are assembled. However, the model of such a stack can be built for the smallest unit

cell, which is expected to depict the response of the whole stack, subjected to the use of proper boundary condition, as reported by Brandon et al. in [60].

Table 1 compares the SOC ASR values obtained with 50% H₂ and 50% H₂O fed in the fuel electrode, when the cell operates at 750 °C and under different operating pressures.

As can be seen the ASR obtained from this work compares well with the one obtained by Jensen et al. at all pressures reported. Even if we change composition and compare the ASR reported by Ebbesen et al. [50] we get reasonably good agreement. Table 2 compares the ASR values obtained when the fuel electrode is fed with 10% H₂, 50% H₂O, 45% CO₂, the cell operates at ambient pressure and at different temperatures.

The choice of using the inlet Nernst potential as reference voltage is taken after having checked its accuracy via comparison with the work of Jensen et al. [49]. The resulting voltages are reported in Table 3 for a SOC operated at 750 °C, at several pressures, fed with different compositions at the fuel electrode, and with pure oxygen at the air electrode.

To evaluate the reliability of our model, the IV curves obtained from it are compared with the reproduction of the IV curves experimentally obtained from the work of Jensen et al. [49]. Results are illustrated in Fig. 2, for different pressures and different fuel electrode composition, when the cell operates in both modes at 750 °C, and with pure O₂ passing over the air electrode.

Similar trends are obtained, and the average relative error when predicting the polarization curves, resulted in a range of 1–3%. From the IV curves and the ASR values obtained we can conclude that the model provides good agreement with existing experimental dataset. Slight deviations are observed but these are well within acceptable range for the simulation.

2.1.2. SOFC and SOEC systems configuration and system components (BoP) model

The focus of this paper is not only on SOC stack operating conditions, but also on the analysis of the necessary BoP auxiliary components. The energy production via SOFC is considered for two different scenarios: hydrogen as inlet fuel and syngas as inlet fuel, with the latter case being based on direct internal reforming and the water gas shift reaction assumed to completely convert CO to H₂ [61], due to the favourable operating condition of the stack. The same stack is assumed to work also as steam electrolyser (SOEC) in case of excess of renewable energy.

Initial configurations for SOFC and SOEC systems are shown in Fig. 3. Every system can be divided into different sections, specifically SOC (yellow short dashed line), heat recovery (light blue solid line) and compression sections (red dash-dot line). Furthermore, SOEC systems present a separation section, which is necessary to separate the produced hydrogen from residual steam (grey long dashed line), as well as a heating section (green dotted line).

Environmental conditions are assumed for all plants to be 25 °C (298.15 K) and 1.013 bar (1 atm). All system components are assumed adiabatic. Heat and pressure losses occurring within the necessary pipeline system are neglected. Generally, a pressure drop equal to the 2% of the inlet pressure is chosen for any heat exchanger, ideal heater, afterburner or SOC [62,63]. Compressors are assumed to work constantly at their design point with an isentropic efficiency of 80% and mechanical losses are ignored [48]. In addition, outlet pressure is defined for every compressor. Heat exchangers are assumed to be counter current and adiabatic and are set to maintain the desired outlet temperature of the cold stream. A minimum temperature approach of 20 °C is considered to define temperature ranges in the heat recovery section.

Concerning SOEC systems, external heat sources are modelled through ideal heaters, while an ideal flash separator is used for hydrogen separation. In ideal heaters and the flash separator, no exergy destruction is assumed during heat addition to the process flows [64].

Regarding SOFC systems, only electrical power is considered as the useful product and no electrical losses due to AC/DC conversion or AC generation through synchronous generator are considered.

2.2. Improving system design and performance metrics

The first part of the subsection shortly explains the general strategy followed to enhance the system performance while the second and third parts describe the energy and exergy efficiency analyses of the systems operating in individual as well as bi-directional mode.

2.2.1. Sensitivity analyses of performance to operating parameters and identification of more efficient system configurations

The effect of different system configurations has been studied as means for SOC system efficiencies improvement, and a sensitivity analysis has been carried out to study the effect of the SOC stack parameters (current density, fuel utilisation, and operating temperature) on the system performance and further ameliorate the process chain.

2.2.2. Energy efficiency analysis of individual modes and bi-directional system

2.2.2.1. Energy consideration of SOFC and SOEC stack and systems. Efficiency based on hydrogen or syngas lower heating value (LHV) at 15 °C and 1.013 bar (241.722 MJ/kmol, 184.537 MJ/kmol) is computed for the SOFC and SOEC component, Eqs. (8) and (9) [48,65].

$$\eta_{fc} = \frac{\dot{W}_{fc}}{\dot{n}_{fuel,in} LHV_{fuel}} * 100 \quad (8)$$

$$\eta_{ec} = \frac{\dot{n}_{H_2O,in} U_{Fec} LHV_{H_2}}{\dot{W}_{ec} + \dot{Q}_{ec}} * 100 \quad (9)$$

Heat requirement takes into consideration both entropy change and the irreversibility due to the resistance. Moving from components to system, when the stack is working in SOFC mode, BoP auxiliary power is subtracted from the system power output, to estimate the system net produced power (\dot{W}_{net}). System energy efficiency is achieved dividing this value with the inlet fuel molar flow times the LHV, as expressed in Eq. (10) [48,65]. The heat requirement for preheating the fuel and air to the SOFC operating temperature is taken care of by the heat recovery unit from the outlet streams.

$$\eta_{fc}^{sys} = \frac{\dot{W}_{net}}{\dot{n}_{fuel,in}^{sys} LHV_{fuel}} * 100 \quad (10)$$

In the SOEC systems, the net hydrogen flow between system inlet and outlet ($\dot{n}_{H_2O,in}^{sys} \cdot U_{Fec}$) is multiplied with the LHV and divided with the sum of overall heat and power requirements, Eq. (11) [48,65].

$$\eta_{ec}^{sys} = \frac{\dot{n}_{H_2O,in}^{sys} U_{Fec} LHV_{H_2}}{\dot{W}_{net} + \dot{Q}_{net}} * 100 \quad (11)$$

2.2.2.2. Energy analysis definitions for bi-directional system. The bi-directional system consists of the same stack working in two operating modes, this does not imply that the hydrogen produced

Table 1

Comparison of SOC ASR values obtained experimentally from Jensen et al. in [49] and the ones resulted from our model, with mixture of 50% H₂ and 50% H₂O, at 750 °C and different pressures.

Pressure [bar]	ASR [Ω cm ²]		Δ [Ω cm ²]	REaccuracy [%]
	Jensen et al. [49]	Our model		
1	0.52	0.49	0.03	6
3	0.47	0.47	0	0
10	0.42	0.40	0.2	5

Table 2

Comparison of SOEC experimental ASR values attained from [50] and the numerical values obtained from our model, with mixture of 10% H₂, 50% H₂O, 45% CO₂, at ambient pressure and different temperatures.

Temperature [°C]	ASR [$\Omega \text{ cm}^2$]		Δ [$\Omega \text{ cm}^2$]	REaccuracy [%]
	Ebbesen et al. [50]	Our model		
750	0.51	0.49	0.02	4
800	0.37	0.37	0	0
850	0.26	0.27	0.01	5

Table 3

Comparison of $V_{NST,in}$ calculated via our model and the OCV experimentally measured in [49].

Fuel electrode composition	Pressure [bar]	OCV [V]	$V_{NST,in}$ [V]	Δ [V]	REaccuracy [%]
80%H ₂ , 20% H ₂ O		Jensen et al. [49]	Our model		
	1	1.037	1.052	0.015	1.4
	3	1.062	1.077	0.015	1.4
	10	1.084	1.103	0.019	1.7
50%H ₂ , 50% H ₂ O		Jensen et al. [49]	Our model		
	1	0.969	0.992	0.023	2.3
	3	0.996	1.015	0.019	2
	10	1.011	1.042	0.031	3

from the stack when working as an electrolyser fulfil exactly the total hydrogen requirement for the stack when working as a fuel cell.

The Bi-SOC system efficiencies are designed as follows:

$$\text{If } \dot{E}_{SOEC} > \dot{E}_{SOFC}, \quad \eta_{Bi-SOC} = \frac{\dot{W}_{net,SOFC} + \dot{E}_{SOEC} - \dot{E}_{SOFC}}{\dot{W}_{net,SOEC} + \dot{Q}_{net,SOEC}} \quad (12)$$

$$\text{If } \dot{E}_{SOEC} < \dot{E}_{SOFC}, \quad \eta_{Bi-SOC} = \frac{\dot{W}_{net,SOFC}}{\dot{W}_{net,SOEC} + \dot{Q}_{net,SOEC} + \dot{E}_{SOFC} - \dot{E}_{SOEC}} \quad (13)$$

$$\text{If } \dot{E}_{SOEC} > \dot{E}_{SOFC}, \quad \eta_{Bi-SOC} = \frac{\dot{W}_{net,SOFC}}{\dot{W}_{net,SOEC} + \dot{Q}_{net,SOEC}} \quad (14)$$

where $\dot{E}_{SOEC} = \dot{n}_{H_2O,inSOEC} \cdot U_{Fc} \cdot LHV_{H_2}$ and $\dot{E}_{SOFC} = \dot{n}_{fuel,inSOFC} \cdot LHV_{fuel}$. When the energy content of the hydrogen produced by the electrolyser system is higher than the energy content of the fuel input to the SOFC, net chemical energy is produced by the bi-directional SOC system in addition to the net power produced by the fuel cell system. When the energy content of the fuel input to the SOFC is higher than the energy content of the H₂ produced via SOEC, net chemical energy needs to be added to the overall.

2.2.3. Exergy efficiencies analysis on individual modes and bi-directional system

2.2.3.1. Exergy considerations for SOFC and SOEC stack and systems. The general steady state exergy balance is applied to every system component. Only chemical and thermomechanical exergy are calculated and taken into account. The Baher state is chosen for this work [47].

Electrical work is pure exergy, while exergy of heat depends on temperature. Moving to exergy efficiency, the exergy source and product terms can be defined for every component. These are used within the functional exergy efficiency definition, which is the ratio between the defined exergy product to the defined exergy source. Total exergy variation (out-in) is used as SOFC exergy source, as well as SOEC product. These differences are computed using stream values at SOC component outlet and inlet.

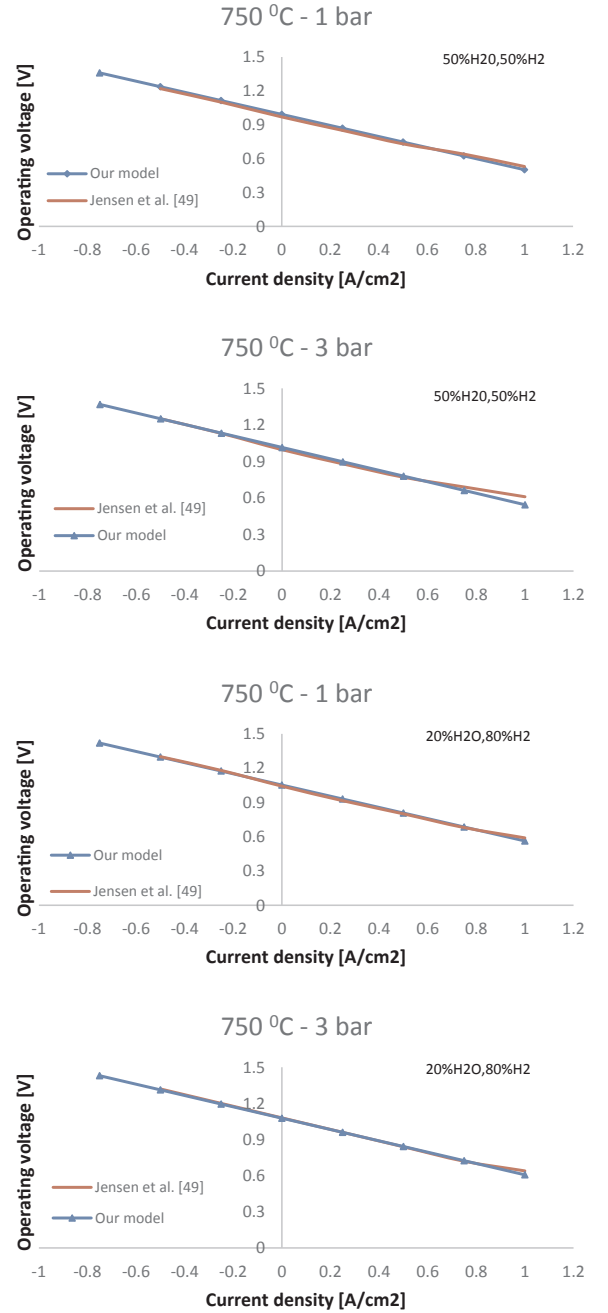


Fig. 2. Comparison of SOC IV curves obtained experimentally from the work of Jensen et al. [49] and numerically from our model.

The electrical work is then used as SOFC product and SOEC source. Heat exchangers have the total exergy change at the hot side (in-out) and total exergy change at the cold side (out-in), being respectively source and product terms. No exergy destruction is assumed for ideal heaters and flash separators.

The exergy destruction for a component is estimated using the Eq. (15) [64,65].

$$Ex_D = \Sigma(\dot{n}_{k,in} ex_{k,in} - \dot{n}_{k,out} ex_{k,out}) - \dot{W} + Ex_Q \quad (15)$$

Fuel cell system source is the fuel (H₂ or syngas) chemical exergy input, while net power is the useful product (\dot{W}_{net}) as in Eq. (16) [64,65]. Conversely for SOEC, the useful product is the net chemical exergy increase between hydrogen outlet flow from the flash separator

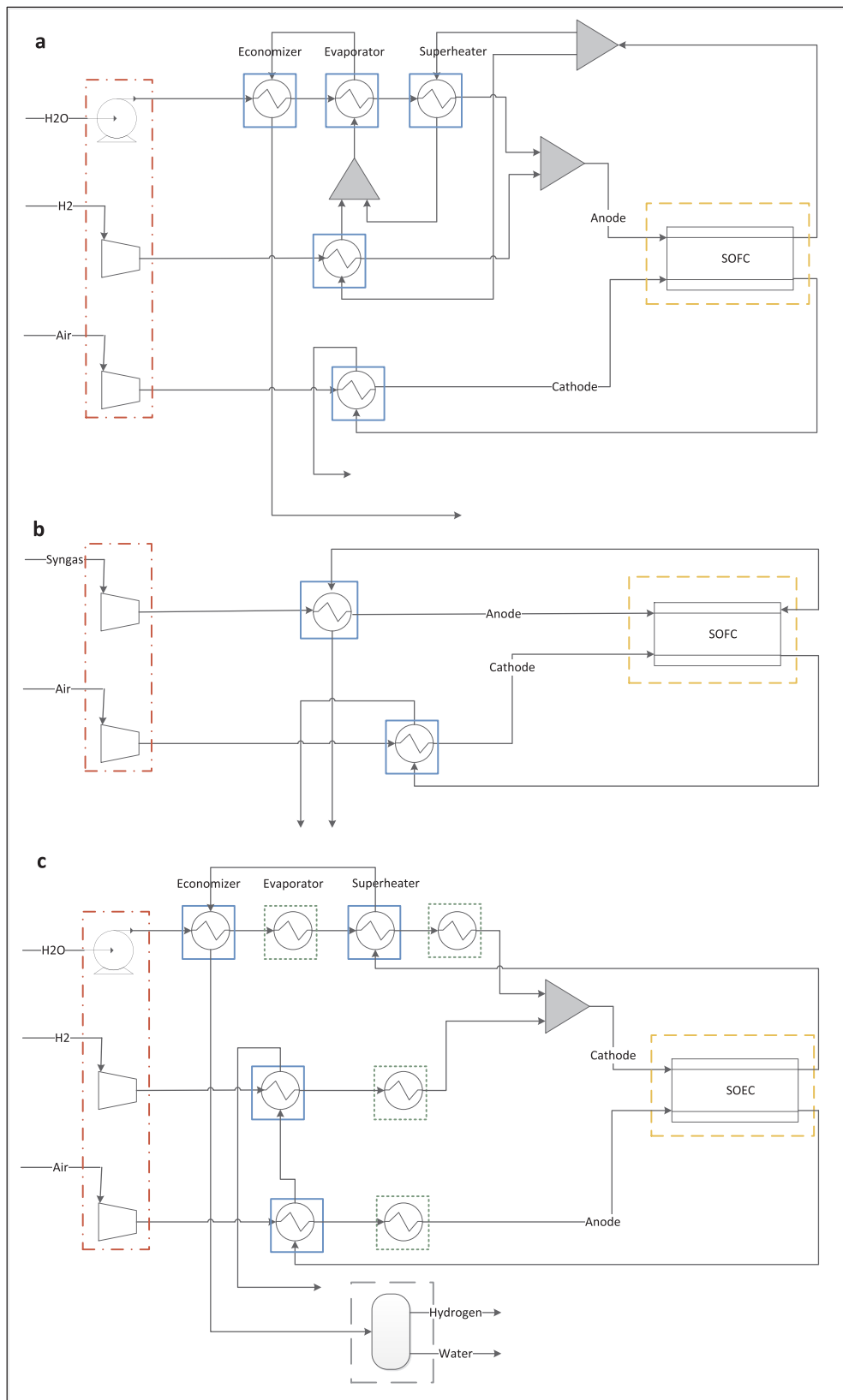


Fig. 3. (a) SOFC system configuration with H₂ as inlet fuel. (b) SOFC system configuration as syngas as inlet fuel, and (c) SOEC mode system configuration. Compression section is highlighted in red (dash-dot line), heat recovery section in light blue (solid line), the ideal heating unit in green (dotted line). (For interpretation of the references to colour in this figure legend, the reader is referred to the web version of this article.)

and hydrogen inlet flow. Exergy sources are the overall net power and heat exergy provided to the system as illustrated in Eq. (17) [64,65]. The chemical exergy change due to oxygen production is not included among the exergy product, thus it is a loss.

$$\eta_{EX,fc}^{sys} = \frac{\dot{W}_{net}}{EX_{fuel,in}} \quad (16)$$

$$\eta_{EX,ec}^{sys} = \frac{EX_{H_2,out} - EX_{H_2,in}}{\dot{W}_{net} + EX_{Qnet}} \quad (17)$$

2.2.3.2. Year-round cumulative exergy losses on bi-directional system

2.2.3.2.1. Rationale and definition. In a Bi-SOC system the same SOC stack operates as both energy storage and power generating device, based on the energy demand and production. However, as explained in the previous section, SOEC and SOFC system have their own different efficiencies and exergy losses. Although the two systems have similar BoP components, their contribution to the exergy destruction varies based on the operating scenario. The year-round CE method is introduced to identify more accurately the process steps responsible for the largest exergy losses and to more effectively optimise the process flow chart. This method takes into account the yearly operational hours of the Bi-SOC system in both the fuel cell and electrolysis mode individually. Based on the operational hours, the exergy analysis is carried out for SOFC and SOEC systems evaluating all individual chain components contribution and those components causing the highest yearly exergy destruction are the target of the optimisation.

Based on the operating regime in a year, the off-design parameters of a system may vary and this could be incorporated in the year-round CE analysis to obtain a more accurate idea of the exergy flow in the system. However, in the present study, the system is assumed to operate at design conditions. The assumption is a simplification of real operating conditions. Nonetheless, this approach might be accurate when a number of smaller systems are used in parallel to meet the varying loads. In fact, some of the systems can be switched on or off but the working ones will be operated at design conditions.

The SOC system exergy efficiency is calculated as the ratio of the final exergy product and final exergy source in a year. For the SOC system, the exergy product when working as electrolyser is the difference between the exergies of the outlet hydrogen stream and the inlet hydrogen stream, while when working as fuel cell the exergy product is the net power produced. The SOEC exergy source is the sum of net power requirement and exergy of the heat requirement while the SOFC exergy source is the exergy of the inlet fuel stream.

Similarly to the system energy efficiency calculation mentioned before, the Bi-SOC system CE efficiency is calculated as reported in Eqs. (18) and (19), with t_{SOFC} and t_{SOEC} being the yearly operational hours of the system in the two individual modes.

$$\begin{aligned} \text{If } EX_{in,SOFC} \cdot t_{SOFC} > EX_{out,SOEC} \cdot t_{SOEC} \quad \eta_{EX_{Bi-SOC}}^{CE-sys} \\ = \frac{EX_{P,SOFC} \cdot t_{SOFC}}{EX_{S,SOEC} \cdot t_{SOEC} + EX_{S,SOFC} \cdot t_{SOFC} - EX_{P,SOEC} \cdot t_{SOEC}} \quad (18) \end{aligned}$$

$$\begin{aligned} \text{If } EX_{in,SOFC} \cdot t_{SOFC} > EX_{out,SOEC} \cdot t_{SOEC} \quad \eta_{EX_{Bi-SOC}}^{CE-sys} \\ = \frac{EX_{P,SOFC} \cdot t_{SOFC} - EX_{S,SOFC} \cdot t_{SOFC} + EX_{P,SOEC} \cdot t_{SOEC}}{EX_{S,SOEC} \cdot t_{SOEC}} \quad (19) \end{aligned}$$

2.2.3.2.2. Estimation of the operational hours for the individual modes. In order to apply the CE method, the yearly operational hours of the SOC in both modes has to be pinpointed. In this work, the estimation is based on a literature review of the foreseen Dutch energy demand and production. Based on [66], the Dutch average excess capacity in 2020 will be 2060 MW. In the same year, a total of 2 TWh of excess electricity will be available over the year. This electricity will be available for a total duration of 984 h in a year. In the year 2050, a total

of 27.6 TWh of excess electricity will be available over the year with an average excess capacity of 7130 MW. The amount in excess will increase significantly leading to 3950 h per year.

In this analysis, the bi-directional SOC will operate 984 h in electrolysis and 7776 h in fuel cell mode considering the installation in the year 2020. In the year 2050, the system will work 3950 h and 4810 h in SOEC and SOFC, respectively.

2.3. Bi-directional system and stack operating conditions: Base-case assumptions

Parameters selection for system analysis involves the stack inlet and outlet temperatures, pressure, current density, fuel utilisation, and inlet composition. A study with starting set of parameters termed as *base-case* is presented. Considering the *base-case*, an *improved-case* is then proposed after a detailed sensitivity analysis of the stack parameters and their influence on the system efficiency.

Here the values of these parameters, for the scenario henceforth named *base-case* are reported:

- Utilisation factor of steam (UF_{ec}) or Utilisation factor of fuel (UF_{fc}) = 0.75 [67]
- SOC Inlet temperature (T_{in}) = 800 °C [40,42–44]
- Inlet pressure (p_{in}) = 1.2 bar for the atmospheric case and 10 bar for the pressurised case [43,44,49]

The fuel/steam electrode inlet compositions (γ_{in}) are kept the same for *base-case* and *improved-case* and are reported in Table 4 [47,68–70], the flow rate of syngas of 0.141 kmol/s is determined such that the equivalent flow rate of hydrogen in the inlet stream is 0.11 kmol/s.

Hydrogen oxidation and steam electrolysis are studied at 800 °C. An absolute temperature difference of 100 °C is assumed over the SOC component. The SOEC is modelled in endothermic mode. Air composition is on molar basis 21% oxygen and 79% nitrogen.

SOFC_{H2} atmospheric systems is designed to operate at a typical voltage 0.75 V [48] with a power output of 12 MW. The resulting current density (8204 A/m²) is used as an input in the SOFC_{syngas} and SOEC configurations. Table 5 shows inputs and outputs for both SOFC and SOEC systems.

3. Analysis and results for individual modes

3.1. SOC Base-case system results (energy and exergy analysis)

Both energy and exergy analysis has been carried out for the three *base-cases* illustrated in Fig. 3. Main results are summarised in Table 6, and in the following section, for SOFC H₂-based, SOFC syngas-based, and SOEC configurations.

The SOFC_{H2} component efficiency based on Eq. (8) is ~44% while

Table 4
Inlet compositions of fuel/steam electrode and their respective flow rates.

Component	SOFC _{H2}		SOFC _{syngas}		SOEC	
	Flow rate [kmol/s]	Mole fraction [%]	Flow rate [kmol/s]	Mole fraction [%]	Flow rate [kmol/s]	Mole fraction [%]
H ₂ O	0.01	10	0.047	33	0.11	90
H ₂	0.11	90	0.038	27	0.01	10
CH ₄			0.011	8		
CO			0.028	20		
CO ₂			0.017	12		
Total flow [kmol/s]	0.12		0.141		0.12	

Table 5
Inputs and outputs for SOFC and SOEC systems.

System	Input	Output
SOFC _{H2}	$V = 0.75$; $\dot{W} = 12$ MW	$\dot{n}_{H_2,in} = 0.11$ kmol/s; $A = 1950.38$ m ²
SOFC _{syngas}	$\dot{n}_{syngas,in} = 0.14$ kmol/s; $A = 1950.38$ m ²	$V = 0.68$; $\dot{W} = 10.9$ MW
SOEC	$\dot{n}_{H_2O,in} = 0.11$ kmol/s; $A = 1950.38$ m ²	$V = 1.142$; $\dot{W} = 18273.25$

when working with syngas as a fuel the SOFC_{syngas} stack efficiency reaches $\sim 42\%$ with a current density of 8204 A/m² and 10902 kW electric power produced. When at atmospheric conditions, in SOFC_{H2} mode, the overall system energy and exergy efficiencies are $\sim 40\%$ and $\sim 41\%$ while in the SOFC_{syngas} scenario the total energy and exergy efficiency are ~ 3 and ~ 5 percentage points less, reaching $\sim 37\%$ and $\sim 36\%$, respectively. Also in the syngas scenario, despite the endothermic nature of the methane reforming reaction, the heat generated by the process is extremely high and hence the air requirement to cool down the cell is large. Correspondingly, in both hydrogen and syngas case, the compression requirement for the inlet air is the major auxiliary energy intake of the systems decreasing their efficiency significantly. The heat transfer is the main cause of exergy destruction in both cases.

The SOEC current density is 8204 A/m² and the power requirements of SOEC is $18,273$ kW, with a voltage of 1.142 V. The SOEC configuration energy and exergy efficiencies are $\sim 76\%$ and $\sim 86\%$. The thermal power required to heat up the inlet streams of the stack leads to dominant auxiliary energy consumption. The stack is the limiting exergy component in this scenario. The exergy destruction fractions of the individual components in the SOEC systems are shown in Fig. 4. The EX_D nominal values in kW are reported in Table 7.

In accordance with literature [17,18,20,47,48,51,69], internal heat transfer and SOEC stack contribute to a high rate of the inlet plant exergy. The exergy analysis illustrates that the internal heat exchange has the greatest exergy destruction rate, followed by the stack that also heavily contributes to the total irreversibility. Also, atmospheric SOEC systems in the literature present energy and exergy efficiency generally between 40% and 60% in fuel cell mode [50,61] and between 60% and 80% in electrolysis mode [28,71].

3.2. System configuration analysis and influence of operating parameters

In this subsection, the results of the different enhancement strategies investigated are presented. From the base-case systems analysis, the large cooling air requirement resulting in high outlet air exergy indicates scope for optimisation. Therefore, Section 3.2.1 illustrates the results obtained by adding air recirculation to the SOFC system when fuelled with syngas. In the second part the SOFC and the SOEC systems are evaluated when operated in pressurized conditions and the SOFC system with the further addition of a gas turbine bottoming cycle for both the H₂-fuelled and the Syngas-fuelled case. Two system

configurations for adding the gas turbine to the exhaust of the pressurised SOFC are analysed. These measures are expected to decrease the exhaust exergy loss and the exergy destruction due to heat transfer. The third subsection contains the results of the sensitivity analysis on SOFC stack parameters and how they influence the performance of the whole systems. This analysis was executed to decrease the exergy loss in the stack component. The final subsection summarises the results of the different system configurations and the influence that operating key parameters have on the system performance.

3.2.1. Air recirculation configuration

Current densities have significant impact on fuel cell performance with higher efficiency at lower current densities. Furthermore, the air requirement can be reduced by operating the fuel cell at lower current densities since lower heat production leads to a lower cooling air flow, and therefore system compression duty requirements are also reduced. However, when operating the SOEC stack in electrolysis mode, different current densities can lead to completely different results. Higher exergetic efficiency can be achieved at high operating current density. Nevertheless, current density determines the difference between operating voltage and thermoneutral voltage. The thermoneutral voltage is defined as the voltage at which the Joule heat generated by the loss of the reactions in the cell and the heat consumption for the electrolysis reaction are equal, which means that the electrical energy input equals the enthalpy of reaction [72,73].

If the cell is operated below thermoneutral voltage, i.e. in the endothermic mode, the electric energy input is below the enthalpy of reactions. When operating at lower current densities in this region more heat must be supplied to the stack to perform electrolysis and to maintain the temperature. Conversely, if the voltage is higher than thermoneutral, i.e. exothermic mode, the electric energy input exceeds the enthalpy of the reaction. In this region growing current densities lead to higher air flow necessary to cool the SOEC.

Another possible option to boost the temperature of the air exiting the compressor at SOEC inlet level, and which might reduce significantly the air compression requirement, is the cathode air recirculation. Essentially, the exergy destruction due to heating the inlet exergy stream in the SOFC_{syngas} system is about $\sim 20\%$ and the exergy loss in the outlet exergy stream is $\sim 44\%$. Therefore, the system can be improved via partially recovering the outlet exergy stream. Cathode air recirculation is implemented at the SOFC_{syngas} system and its effect is described in this section. Similar to the approach used in literature [51,64,74], the stack assumptions and the operating conditions remain the same, and the fraction recirculated is determined such that the cathode inlet temperature is kept at the SOFC inlet nominal temperature, in our case 800 °C. Nernst voltage for the air recirculation configuration slightly decreases accordingly with the reduction of oxygen partial pressure in the cathode stream. The electric power produced reduces by ~ 64 kW. Nevertheless, the system net work increases since the air compression work reduces from 1297 kW to 411 kW. The system energy and exergy efficiencies increase by 3 percentage points reaching $\sim 40\%$ and $\sim 39\%$, respectively. The exergy destruction in the air compressor and internal heat exchanger decrease significantly, in

Table 6
Inputs and outputs (in shaded cells) for SOFC and SOEC systems for the base-case scenario.

	SOFC H ₂ -based	SOFC syngas-based	SOEC
Pressure	1.2 bar	1.2 bar	1.2 bar
T _{in}	800 °C	800 °C	800 °C
T _{out}	900 °C	900 °C	700 °C
Area	1950.38 m ²	1950.38 m ²	1950.38 m ²
UF_{fc}, UF_{ec}	0.75 mol/mol	0.75 mol/mol	0.75 mol/mol
J	8203.58 A/m ²	8203.58 A/m ²	8203.55 A/m ²
\dot{W}	12 MW	10.9 MW	18.2 MW
V	0.75	0.68 V	1.14 V
$\eta_{sys,SOFC} / \eta_{sys,SOEC}$	40 %	37 %	76 %
$\eta_{EX,fc}^{sys} / \eta_{EX,ec}^{sys}$	41 %	36%	86%

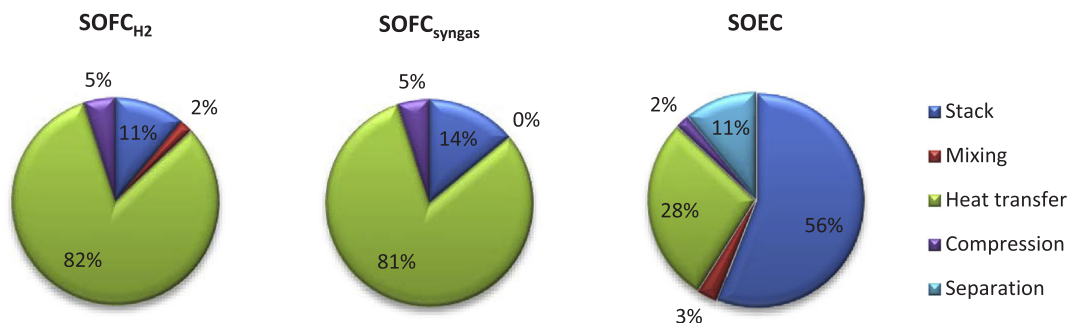


Fig. 4. Exergy destruction fraction of the individual components in the SOC systems.

Table 7

Exergy destruction values of the individual components in the SOC systems.

Component	$EX_{D,SOFC_{H_2}}$ [kW]	$EX_{D,SOFC_{syngas}}$ [kW]	$EX_{D,SOEC}$ [kW]
Stack	600	741	1593
Mixer	108	-	99
Internal heat exchangers	4700	4289	794
Compressors and Pump	278	265	59
Separator	-	-	302
Total	5686	5295	2847

accordance with [51,64,74]. Fig. 5 and Table 9 illustrate the exergy destruction fractions and the exergy destruction kW values of the individual components in the two different scenarios.

Anode recirculation might also help in further enhancing the system performance. However, when syngas is fed to the stack, the outlet stream is rich in $H_2O(g)$ and CO_2 and has a very low concentration of CO and H_2 , leading also to a significantly reduced open circuit voltage. Hence, anode recirculation is not considered in the scenario where the SOFC is fuelled with syngas. Nonetheless, the anode outlet stream can be used as a source of high temperature heat, being approximately at 400 °C.

The outlet stream exergy losses can be diminished also integrating the system at pressurized conditions with a gas turbine bottoming cycle. Next section discusses the modelling of this scenario and its effect on system performance.

3.2.2. Pressurized SOC individual systems and implementation of the turbine bottoming cycle

3.2.2.1. SOFC and SOEC pressurized condition. The two base systems, SOFC fed with H_2 and SOEC working as steam electrolyser are evaluated in pressurized condition. Both fuel cell and electrolyser SOCs show a decrease in the internal resistance with increasing pressure from $3.64 \cdot 10^{-5}$ to $3.01 \cdot 10^{-5} \Omega m^2$, while the Nernst potential increases by 0.05 V reaching 0.89 V.

Pressurizing the SOEC has no significant effect on the stack heat and the electric power requirement. However, the auxiliary work required to compress the air increases drastically from 306.78 kW to 5672.30 kW leading to system energy efficiency of ~64%, 12 percentage points less than in the corresponding atmospheric configuration. When at 10 bar, the exergy efficiency is ~70% as compared to 86% of the atmospheric scenario. Nonetheless, pressurized operation has the advantage of producing pressurized H_2 which might improve the complete process chain efficiency, especially in presence of a gas upgrading process or pressurized storage [71].

Also the SOFC pressurized scenario results in a lower system performance. In fact, even though SOFC component efficiency is ~45% for both atmospheric and pressurized cases, when operated at 10 bar the SOFC system is inefficient since the auxiliary compression on work is

larger than the produced SOFC power. This is in agreement with literature [51,64]. Nonetheless, in previous work, pressurized SOFC systems have been shown to be highly efficient when combined with a bottoming Gas Turbine (GT) cycle [75].

In both systems, pressurization affects the heat recovery sections modifying the water saturation temperature, product gas dew point temperature and air temperature at the inlet of the heat recovery section. As a consequence, higher system outlet temperature might emerge. Hence, having system outlet streams at higher temperature and pressure, a higher fraction of input exergy is lost at system outlet in the form of thermo-mechanical exergy. This exergy could be partially recovered through the addition of a gas turbine at the outlet, as done in different work [76].

3.2.2.2. SOFC scenario with integrated gas turbine, two expansion system configurations. To take advantage of the exergy available at the SOFC stack outlet and decrease the exhaust exergy loss, a Gas Turbine bottoming cycle is added to the system. The performance of the integrated SOFC-GT system is evaluated at 800 °C and 10 bar for both hydrogen and syngas case. The system components in addition to the earlier components include an afterburner and a gas turbine. The afterburner is modelled using a stoichiometric reactor. The reactor is adiabatic, thus resulting in an increased temperature of the stream at the outlet of the afterburner.

Two different configurations, illustrated in Fig. 6, are studied and compared in terms of energy and exergy efficiencies. As in literature [51,77,78], the cathode air side split fraction in both configurations is set to maintain the cathode inlet temperature, in our case 800 °C. The gas turbine in both cases is modelled with pressure ratio 0.125 [64], isentropic efficiency 90% and mechanical efficiency 100%. The anode heat exchanger is modelled to raise the anode inlet temperature to 800 °C whereas the cathode heat exchanger is set such that the difference between the hot inlet stream and cold outlet stream is 20 °C.

In configuration 1 the turbine inlet temperature is lower than the output temperature of the afterburner because of the heat recovery unit with the inlet syngas stream. However, since increasing the turbine inlet temperature (TIT) increases the power output of the turbine [77], configuration 2 is implemented with an effort to increase the turbine

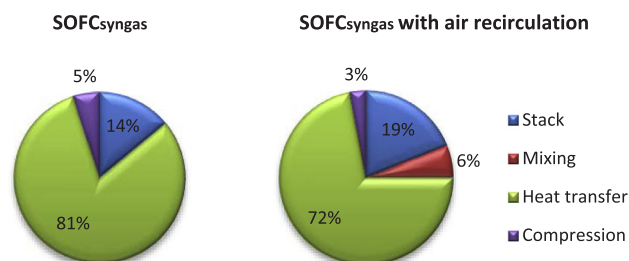


Fig. 5. Exergy destruction fraction of the individual components of the SOFC system with and without air recirculation.

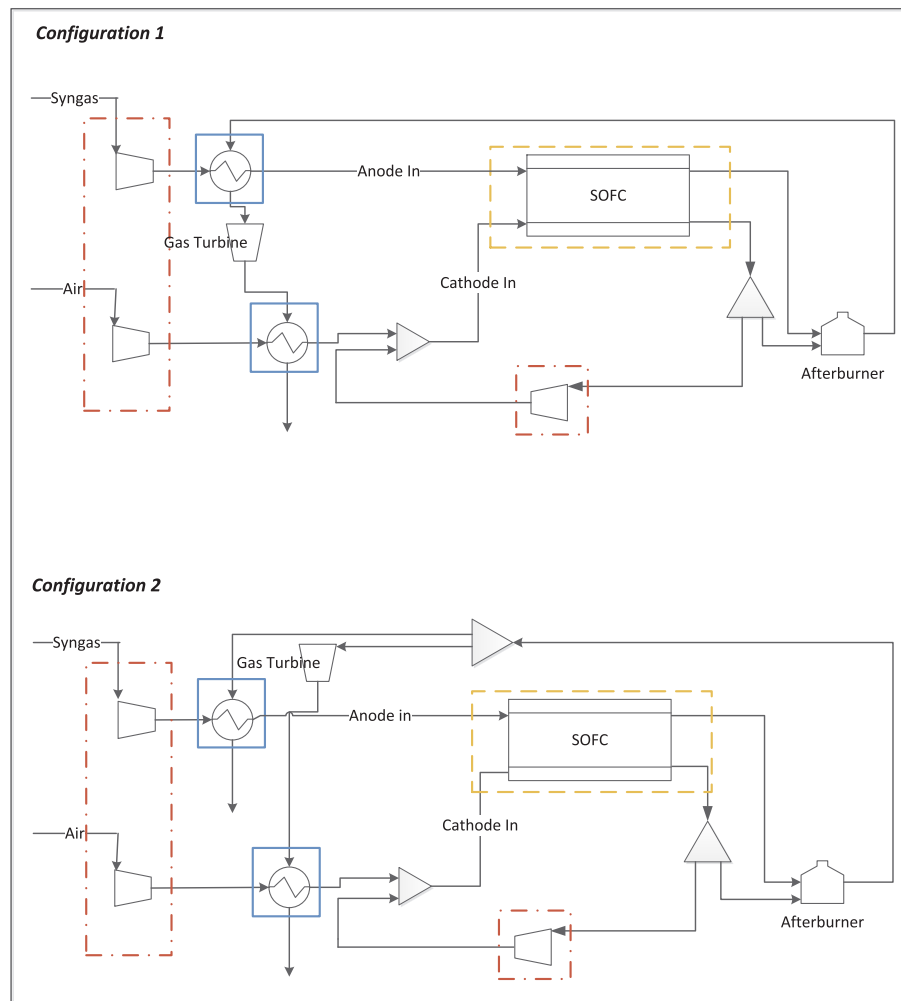


Fig. 6. The two different expansion system configurations adopted to integrate the gas turbine with the SOFC_{syngas} system.

inlet temperature. The outlet stream of the afterburner is split into two streams such that 90% of the flow is let to the gas turbine while 10% flows to the anode heat exchanger to avoid the need of external heat source to partly preheat the anode stream.

When the stack is fed with syngas, the GT power produced increases from 13,062 kW in *configuration 1* to 13,163 kW in *configuration 2*. However, due to the different recirculation split factors, the partial pressure of oxygen at the cathode differs thereby changing the electric and thermal power generated by the fuel cell. The cathode inlet air flow rate required in *configuration 2* (0.73 kmol/s) is larger than in *configuration 1* (0.66 kmol/s), thereby increasing the required air compression power of ~670 kW. Ultimately, *configuration 2* provides a lower total power output resulting in a system energy efficiency ~62%, ~2 percentage points lower than that of *configuration 1* (~64%). Similarly, the system exergy efficiency for *configuration 2* (~60%) is lower by about ~2 percentage points than in *configuration 1*. For this reason the further analyses focuses only on *configuration 1*.

Thanks to the gas turbine integration, extra power is produced, increasing the net power generated by the system by ~75%. The system energy efficiency increases by ~27 percentage points from the *base-case*, and ~24 percentage points from the case with air recirculation. At higher pressure, the internal losses are lower and the cell voltage increases. Hence, the power generated by the stack increases by ~1350 kW, leading to ~5 percentage points higher stack efficiency. The system exergy efficiency increases significantly as well reaching ~62%. The energy and exergy performance of the SOFC systems, when it is fed with syngas, are summarized in Table 8, conforming to [18,64].

The integration with the GT reduces the system exergy losses from 45% to 21% of the system inlet exergy. The exergy analysis, in line with literature [50,61,76], shows an enhanced exergetic performance for the pressurized scenario with GT, a better use of hot product gas for additional preheating treatment, and a lower rate of exergy destruction. The exergy destruction fractions are shown in Fig. 7.

Table 8
SOEC systems performance of the SOFC systems when fed with syngas.

	1.2 bar base-case SOFC _{syngas}	1.2 bar base-case SOFC _{syngas} with air recirculation	10 bar base-case SOFC _{GTsyngas}
$P_{elec,fc}$ [kW]	10,903	10,838	12,261
\dot{W}_{comp}^{syngas} [kW]	108	108	1797
\dot{W}_{comp}^{air} [kW]	1297	412	6708
$\dot{W}_{comp}^{air,recirc}$ [kW]	-	-	291
\dot{W}_{GT} [kW]	-	-	13,063
\dot{W}_{net} [kW]	9497	10,319	16,528
$EX_{syngas,in}$ [kW]	26,598	26,598	26,598
$EX_{total,in}$ [kW]	26,830	26,672	26,667
$EX_{syngas,out}$ [kW]	9817	9809	5499
$EX_{total,out}$ [kW]	12,038	12,432	5499
EX_D [kW]	5296	3922	4642
$\eta_{sys,SOFC}$ [%]	~37	~40	~64
$\eta_{EX,fc}^{sys}$ [%]	~36	~39	~62

Table 9

Exergy destruction kW values of the SOFC components system with and without air recirculation, and in pressurized conditions with GT integration.

Component	$EX_{D,SOFCSyngas}$ with air recirculation [kW]	$EX_{D,SOFCSyngas}$ [kW]	$EX_{D,SOFCSyngas}$ -GT Configuration1 [kW]
Stack	745	741	604
Mixer	235	-	186
Internal heat exchangers	2824	4289	743
Compressors and Pump	118	265	836
Gas Turbine	-	-	464
Combustor	-	-	1810
Total	3922	5295	4643

For the system running with H_2 as fuel, the GT leads the system energy efficiency to increase from $\sim 40\%$ to $\sim 68\%$. When the SOFC is combined with the GT, the higher compression work (8347 kW compared to 1650 kW) is balanced by a lower overall exergy destruction rate (3527 kW compared to 5686 kW) and higher electrical output (26,436 kW compared to 12,000 kW). As a consequence, the system exergy efficiency also rises to $\sim 70\%$, as compared to the $\sim 41\%$ obtained in the stand-alone system.

In line with literature, even though exergy destruction due to turbine and burner addition is introduced, overall system exergy efficiency is higher due to a better utilisation of the outlet exergy [16–18,51,78]. Specifically, the large reduction in heat transfer losses indicates the advantage of internal heat transfer through anode and cathode recirculation. Fig. 8 and Table 10 show the exergy destruction fraction of the different components in the various $SOFCH_2$ configurations.

3.2.3. Sensitivity analysis on stack parameters and their influence on the performance of the systems

Reduction in the stack exergy destruction might further improve the system performance. Reduction in the stack exergy destruction might further improve the system performance. For this reason, a sensitivity analysis on the SOFC syngas stack operating parameters (i.e., fuel cell current density, UF, temperature) is carried out to present the energetic and exergetic performance. During each sensitivity analysis, only one parameter is varied while the remaining assume their base case values. The choice of optimising only the SOFC system is due to the expected operational hours of the bi-directional system. In fact, while in 2050 the expected operation time is almost the same between the two operating modes, in 2020 the system is expected to operate for almost the 90% of the time in SOFC mode.

The stack surface area is taken as 1950.38 m^2 and the inlet molar flow has been varied between 0.064 kmol/s and 0.166 kmol/s (leading to current density of 3710.16 A/ m^2 and 9646.41 A/ m^2 , respectively). At high current density we expect an increase in the waste heat, therefore the current density range is selected for achieving high stack efficiency

at lower current density and improving system thermal management.

The stack temperature is also a primary factor in determining the electrochemical performance because of its influence on the ohmic resistance of the solid electrolyte and the kinetics of the charge-transfer reactions. Temperature has been varied between 700 °C and 900 °C.

The fuel utilisation also affects the system performance through stack electrical performance and thermal characteristic. However, in order to avoid a significant increase in the cathode concentration over potential due to steam usage near the cell outlet, it is extremely important to keep the UF within certain limits [79]. For this reason, finally, while keeping the operating temperature at 800 °C for the above current densities the utilisation factor has been varied between 0.65 and 0.85.

3.2.3.1. Effect of temperature, current density and utilisation factor on stack performance. Looking at temperature variations, it has been seen that higher operating temperatures are favourable due to the corresponding resistance drop but lead to a reduction in Nernst voltage. Nonetheless, the first effect is predominant and the cell operating voltage increases with increasing temperature thereby resulting in more electric power generated and improved stack performance. The same occurs when reducing current density which leads to a lower overvoltage.

When increasing the fuel utilisation, the current density increases and correspondingly the overvoltage thus inducing a lower operating voltage. However irrespective of the decrease in the cell voltage, the SOFC efficiency increases because of a higher output power due to high current density.

3.2.3.2. Comparison of energy and exergy performances of the SOFC system for base-case and improved-case. This subsection illustrates the effect of the parameters selected via sensitivity analysis on the performance of the atmospheric and pressurized with GT scenarios. This set of parameters, henceforth named *improved-case*, have been compared with the results obtained in the *base-case*. Table 11 summarises the parameters that are different in the *base-case* and in the *improved-case*. Both cases are studied for atmospheric and pressurized conditions.

The SOFC system energy efficiency improves by operating the stack more efficiently (i.e., at lower current density, higher temperature and higher fuel utilisation). More precisely, the system performance at atmospheric condition increases by $\sim 18\%$ reaching a system energy efficiency of $\sim 55\%$, while at 10 bar when integrating the gas turbine the system energy efficiency increases from $\sim 64\%$ to $\sim 73\%$. Also the system exergy efficiency increases by ~ 18 percentage points at 1.2 bar and of ~ 9 percentage points when working at high pressure with the GT, reaching $\sim 54\%$ and $\sim 71\%$ respectively, confirming that fuel cell systems are a promising efficient technology for electricity generation. The stack exergy destruction fraction reduces considerably due to reduced current density, from 14% to only 3% at ambient pressure and

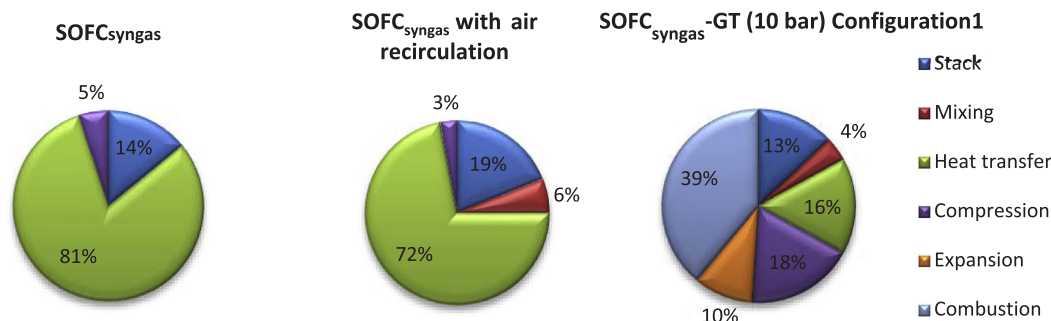


Fig. 7. Comparison of exergy destruction fractions of the individual components of the SOFC Syngas-fuelled system, at atmospheric pressure (base and with air recirculation), and pressurized condition with GT integration.

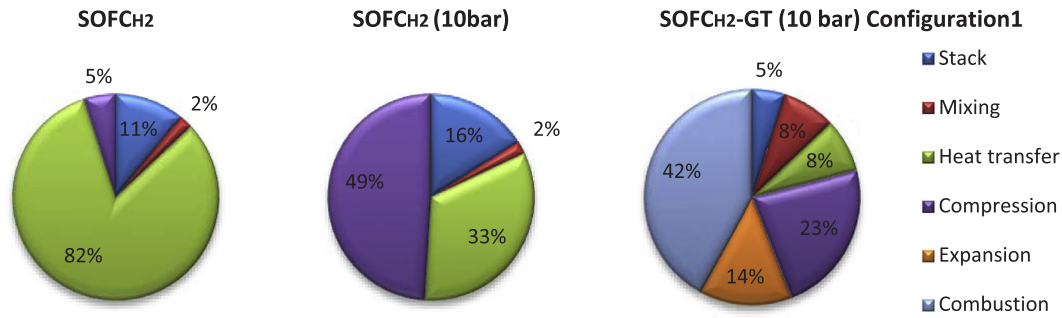


Fig. 8. Comparison of exergy destruction fractions of the individual components of the SOFC H₂-fueled system, at atmospheric pressure and 10 bar, and hybrid configuration.

Table 10

Exergy destruction values of the individual components of the SOFC H₂-fueled system, at atmospheric pressure and 10 bar, and hybrid configuration.

Component	$EX_{D,SOFC_{H_2}}$ [kW]	$EX_{D,SOFC_{H_2}}(10)$ [kW]	$EX_{D,SOFC_{H_2}-GT}$ Configuration1 [kW]
Stack	600	830	162
Mixer	108	113	298
Internal heat exchangers	4700	1720	293
Compressors and Pump	278	2577	797
Gas Turbine	-	-	486
Combustor	-	-	1491
Total	5686	5240	3527

Table 11

Stack operating parameters in the *base-case* and *improved-case*.

Parameters	Base-case	Improved-case
Inlet H ₂ flow rate for SOFCH ₂ /Inlet equivalent H ₂ for SOFC syngas/Inlet steam flow rate for SOEC	0.11 kmol/s	0.05 kmol/s
Operating Temperature	800 °C	850 °C
$UF_{fc/ec}$	0.75	0.85

from 13% to 5% when operated at high pressure and integrated with the GT. Table 12 illustrates a comparison of the performance of the SOFC systems, when fed with syngas, and operating at base-case or improved-case conditions.

3.2.4. Summary of the results in the individual modes

A detailed analysis of steam SOEC system and SOFC system using syngas and H₂ as fuels was presented in the section above. Based on the thermodynamic assessment of the simple schematic of an SOFC system at atmospheric conditions, the exergy lost in the exhaust stream constitutes the major loss while the major exergy destruction occurs in the heat exchangers and stack. To boost the use of hot product gas for additional preheating treatment, the base configuration is modified at atmospheric condition incorporating cathode air recirculation, and at pressurized condition integrating a GT as bottoming cycle. Further improvement is made in the system performance by changing the SOFC parameters current density, temperature and UF. The integration with GT improves the system efficiency drastically reducing the exhaust exergy loss to less than half of the inlet stream exergy. However a negative effect of pressurization is observed in the performance of the SOEC. Pressurization increases the power input required for the SOEC system with very low increase in the output exergy, thus reducing the system energy and exergy efficiency by ~12 percentage points and ~15 percentage points, respectively. An improvement in the system efficiency due to lower cell losses occurs by reducing the current density. Thus, an *improved-case* is simulated considering a lower current

density, from 8203 A/m² to 4205 A/m², increasing the operating temperature from 800 °C to 850 °C and the UF from 0.75 to 0.85. Based on the improved-case, SOFC system efficiency as high as ~73% is obtained when working at high pressure. It can be concluded that SOFC systems have a scope to reach energy efficiencies higher than other power generation processes like combined cycle power plants [80].

4. Results and discussion of bi-directional system

After having seen the individual thermodynamic analysis for SOFC and SOEC systems, the performance of a Bi-SOC system are evaluated to predict its prospects with respect to other energy storage technologies available today.

The analysis is executed on 8 different systems:

1. SOFC_{H₂} + SOEC (SOC_{H₂}); atmospheric pressure; *base-case*
2. SOFC_{syngas} + SOEC (SOC_{syngas}); atmospheric pressure; *base-case*
3. SOFC_{H₂} + SOEC (SOC_{H₂}); atmospheric pressure; *improved-case*
4. SOFC_{syngas} + SOEC (SOC_{syngas}); atmospheric pressure; *improved-case*
5. SOFC_{H₂} + GT + SOEC (SOC_{GT_{H₂}}); pressurized condition; *base-case*
6. SOFC_{syngas} + GT + SOEC (SOC_{GT_{syngas}}); pressurized condition; *base-case*
7. SOFC_{H₂} + GT + SOEC (SOC_{GT_{H₂}}); pressurized condition; *improved-case*
8. SOFC_{syngas} + GT + SOEC (SOC_{GT_{syngas}}); pressurized condition; *improved-case*

The assumptions taken for the atmospheric pressure *base-case* were

Table 12

Energy and exergy results for SOFC systems when the stack is fed with syngas and it operates in *base-case* or *improved-case*.

	1.2 bar base-case SOFC _{syngas}	1.2 bar improved-case SOFC _{syngas}	10 bar base-case SOFC _{GT_{syngas}}	10 bar improved-case SOFC _{GT_{syngas}}
$P_{elec,fc}$ [kW]	10,903	6955	12,261	7269
\dot{W}_{comp}^{syngas} [kW]	108	48	1797	813
\dot{W}_{comp}^{air} [kW]	1297	458	6708	2008
$\dot{W}_{comp}^{air,recirc}$ [kW]	-	-	291	110
\dot{W}_{GT} [kW]	-	-	13,063	4208
\dot{W}_{net} [kW]	9497	6449	16,528	8546
$EX_{syngas,in}$ [kW]	26,598	12,029	26,598	12,029
$EX_{total,in}$ [kW]	26,830	12,111	26,667	12,050
$EX_{syngas,out}$ [kW]	9817	3357	5499	2203
$EX_{total,out}$ [kW]	12,038	4087	5499	2203
EX_D [kW]	5296	1578	4642	1320
$\eta_{sys,SOFC}$ [%]	~37	~55	~64	~73
$\eta_{EX_{fc}}^{sys}$ [%]	~36	~54	~62	~71

illustrated in Section 2.3. In the pressurised case only the system pressure is modified from 1.2 to 10 bar. The system configuration for the *base-case* and the *improved-case* does not change. Only the operating conditions are different, as previously illustrated in Table 11.

4.1. Bi-directional SOC System, energy comparison on different configurations

Table 13 summarises the Bi-SOC systems energy efficiencies. The SOC systems efficiencies vary from ~29% to ~47% depending on the operating conditions of the stack, systems configuration and inlet fuel.

When fed with syngas, the system is 2.5 percentage points less energetically efficient than when fed with H₂ due to a lower operating voltage since the syngas contain more compounds not involved in the electrochemical reaction. However, the upgrading gas process downstream of the SOC system working with syngas can be more advantageous than when working with H₂. Furthermore, considering the costs and efficiency of the hydrogen production process [81,82] and the difficulties related to its purification, transport and storage, using syngas would be more practical. Moreover, syngas electrochemical conversion can form the link for the integration of the electrical grid and the natural gas infrastructure, addressing in this way one of the key EU energy challenges [83]. The system efficiency when working with syngas is only slightly lower than working with hydrogen maintaining a reasonable initial system efficiency and, therefore, making it a viable option.

By changing the stack parameters in accordance with the *improved-case* the SOFC system efficiency considerably increases. However, this has a negative effect when the stack operates as electrolyser. For the SOEC and in the end for the SOC, the *improved-case* scenario is more efficient when working in atmospheric conditions while the *base-case* scenario turns out to be the best option when working in pressurized condition. In fact, as explained in Section 3.2.1, reducing the current density rises the SOFC system efficiency but reduces the SOEC system efficiency increasing its heat requirement and consequently the auxiliary power need from the SOEC system.

It is therefore more efficient to run the Bi-SOC system using the same stack at higher current densities when operated as electrolyser and at lower current densities when working as fuel cell. Assuming to work the Bi-SOC system in pressurized condition and run the SOFC stack at the operating conditions of the *improved-case* while the SOEC stack under the working conditions of the *base-case* leads to an overall Bi-SOC system efficiency of ~54%.

4.2. ReSOC system configurations comparison, year-round cumulative exergy losses based

Table 14 reports the Bi-SOC systems exergy figures for the years

Table 13
Bi-SOC systems energy efficiencies.

	1.2 bar <i>base-case</i>		1.2 bar <i>improved-case</i>		10 bar <i>base-case</i>		10 bar <i>improved-case</i>	
	SOC _{H2}	SOC _{syngas}	SOC _{H2}	SOC _{syngas}	SOC _{GTH2}	SOC _{GTSyngas}	SOC _{GTH2}	SOC _{GTSyngas}
$\dot{W}_{net,SOFC}$ [kW]	10,527	9497.1	7031	6447.1	17986.2	16525.76	9318	8543.3
$\dot{W}_{net,SOEC}$ [kW]	18587.3	18587.3	8144.2	8144.2	24054.6	24054.6	15377.9	15377.9
$\dot{Q}_{net,SOEC}$ [kW]	8010.3	8010.3	8465.3	8465.3	7569.4	7569.4	5338.21	5338.21
\dot{E}_{SOEC} [kW]	20041.2	20041.2	10273.2	10273.2	20041.2	20041.2	10273.2	10273.2
\dot{E}_{SOFC} [kW]	26725.1	26048.0	12084.9	11786.2	26610.7	26,048	12317.3	11786.2
$\eta_{sys,SOFC}$ [%]	~40	~37	~58	~55	~68	~64	~76	~73
$\eta_{sys,SOEC}$ [%]	~76	~76	~73	~73	~64	~64	~50	~50
η_{BI-SOC} [%]	~32	~29	~38	~36	~47	~44	~41	~39

2020 and 2050. In all the cases, the SOEC exergy product resulted lower than the SOFC exergy source; therefore, Eq. (19) is used to calculate the SOC system exergy efficiency.

Since in the year 2020 the SOC system runs for a longer time as a power plant than as an energy storage system, the pressurized *improved-case* is the most efficient alternative. In the year 2050, when the yearly individual operational hours change, the pressurized *base-case* emerges as the most efficient operating option. Fig. 9 illustrates how the Bi-SOC system exergy efficiency varies with the yearly operational hours of the system in fuel cell mode, for the pressurized *base-case* with syngas as fuel. The horizontal axis represents the operational time of the bi-directional system in fuel cell mode, and it is assumed that the stack will work in electrolyser mode for the remaining time of the year. The central vertical line shows the efficiency of the system when the stack works in both mode for equal amount hours. The efficiencies illustrated in the right side of the graph, when the stack works more hour as a power plant, are calculated with Eq. (18), while the efficiencies reported in the left side of the graph, when the stack works more hours as energy storage, are calculated with Eq. (19).

Table 14 and Fig. 9 demonstrate how the Bi-SOC system exergy efficiency is highly affected by the yearly operational hours in both power production and energy storage modes. When $EX_{in,SOFC} \cdot t_{SOFC} = EX_{out,SOEC} \cdot t_{SOEC}$ the exergy efficiency reaches its minimum because the optimal operating conditions for the 2 modes are different.

The exergy analysis identifies the process step with major losses, with the aim of optimising the process flow chart and specifying conditions for Balance-of-Plant components. The process step with major losses are studied through the year-round CE method. Fig. 10 illustrates the exergy flow diagram of the *base-case* Bi-SOC at 10 bar, when the fuel cell is fed with syngas, for the year 2020. All values are CE values and in unit GWh, the losses shown in the diagram are the exergy destruction for the different components, the exhaust loss is the exergy lost to the surroundings via exhaust gas. Table 15 shows the exergy flow fraction of all components as compared to the inlet exergy (215.4 GWh).

A thorough analysis of the foreseen modes of operation of the SOC stack, before the system installation, can significantly improve the optimisation of the process. For example, in a scenario where most of the time the excess of renewable power is higher than the need of electricity, the SOC stack will mostly run in electrolyser mode, consequently under our assumptions the Bi-SOC system must be operated at atmospheric pressure since with this operating conditions the stack can more efficiently convert electricity into hydrogen. This will greatly affect the overall performance of the SOC system.

The year-round CE method helps therefore to predict more accurately what is the most efficient configuration and operating parameters based on the power production and consumption curves.

Table 14
Bi-SOC systems CE efficiencies.

	1.2 bar <i>base-case</i>		1.2 bar <i>improved-case</i>		10 bar <i>base-case</i>		10 bar <i>improved-case</i>	
	SOC _{H2}	SOC _{syngas}	SOC _{H2}	SOC _{syngas}	SOC _{GTH2}	SOC _{GTsyngas}	SOC _{GTH2}	SOC _{GTsyngas}
$Ex_{in,SOFC}$ [kW]	26000.6	26598.6	11759.4	12029.8	26000.6	26598.6	11759.8	12029.8
$Ex_{out,SOFC}$ [kW]	10527.0	9497.1	703	6447.1	17986.2	16525.8	9317.8	8543.3
$Ex_{in,SOEC}$ [kW]	22824.5	22824.5	11623.5	11623.5	28734.4	28734.4	18867.1	18867.1
$Ex_{out,SOEC}$ [kW]	19518.9	19518.9	10004.8	10004.8	20023.9	20023.9	10259.7	10259.7
$\eta_{EX,fc}^{sys}$ [%]	~41	~36	~60	~54	~69	~62	~79	~71
$\eta_{EX,ec}^{sys}$ [%]	~86	~86	~86	~86	~70	~70	~55	~55
$\eta_{EXBI-SOC}^{CE-sys}$ [%] -2020	~40	~35	~59	~53	~67	~60	~73	~65
$\eta_{EXBI-SOC}^{CE-sys}$ [%] -2050	~37	~33	~54	~48	~54	~49	~50	~45

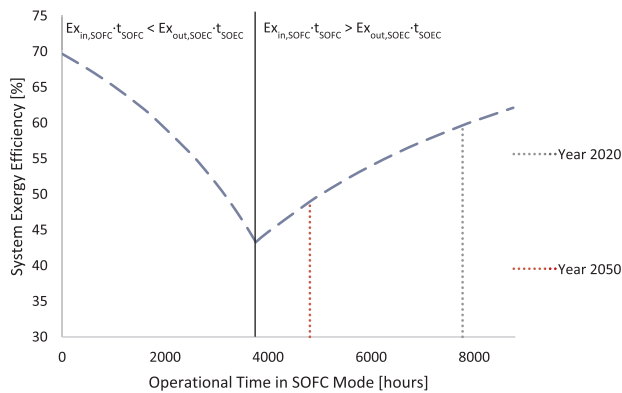


Fig. 9. Variation of the Bi-SOC system exergy efficiency with the operational hours of the system in SOFC mode. Syngas is used as a fuel for the pressurized base-case.

4.3. Further optimisation of bi-directional SOC system, energy and year-round cumulative exergy performance

When working in pressurized condition, 10 bar was chosen to obtain high pressure hydrogen when working in energy storage mode. This can

Table 15
Exergy flow fraction of all components of SOC system as compared to the inlet exergy.

	Component	Fraction [%]
DESTRUCTION	Inlet Exergy	100
	Mixing	0.71
	Heat Transfer	2.96
	Compressor	3.26
	Stack	2.75
	Combustor	6.60
	GT	1.71
	Net destruction	17.99
	Exhaust losses	22.53
	GT P _{EL}	15.40
	SOFC P _{NET}	44.26
	Net Useful Exergy Out	~60

be for further gas upgrading process e.g. methane production process. However, at 10 bar, pressurised operation results energetically demanding due to the high preheating demand when working the electrolyser in the endothermic region. Furthermore, when integrating a GT within a SOFC system, a pressure ratio around 3–5 bar appears more efficient [78].

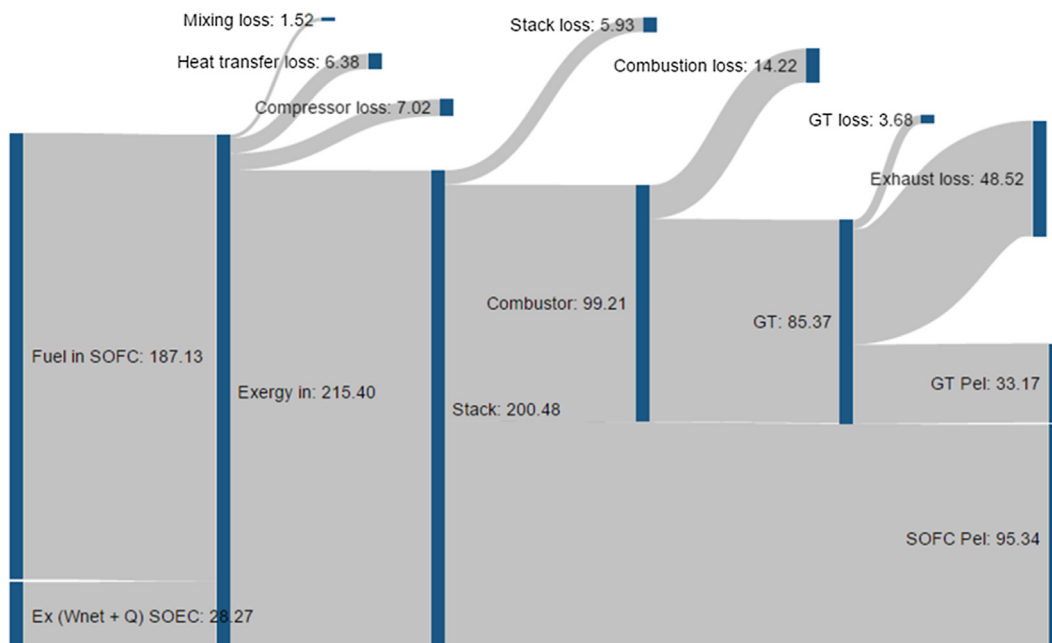


Fig. 10. Exergy flow diagram for the base-case Bi-SOC system at 10 bar when the fuel cell is fed with syngas, during the year 2020. All values are in GWh.

Therefore, the system was also evaluated considering an operating pressure of 4 bar. The air and fuel are compressed to 4 bar, the GT ratio is set to 3.77. When working in electrolyser mode the stack is run at 4 bar and the outlet hydrogen is further pressurized to 10 bar, this compressor is included in the calculation of the system performance.

Reducing the operating pressure decreases the SOFC and the GT electric power produced. However the auxiliary power requirements diminishes as well, leading to an increase of the SOFC system energy efficiency from $\sim 64\%$ to $\sim 66\%$ and SOEC system energy efficiency from $\sim 64\%$ to $\sim 69\%$ in the *base-case*. Due to the high endothermicity of the SOEC and the corresponding large need of air required for heating the stack, the decrease of pressure from 10 bar to 4 bar leads to a decrease in the related auxiliary compression work from 5806.8 kW to 3076.5 kW, including also the compression work required to compress the hydrogen from 4 bar to 10 bar downstream. The overall Bi-SOC system efficiency of the *base-case* at 4 bar increases from $\sim 44\%$ to $\sim 49\%$.

The electrolyser system has been further improved by incorporating air recirculation, with 80% outlet air mass flow rate recirculated to the inlet whereas the remaining 20% is used for preheating the inlet air and hydrogen. The SOEC system energy efficiency rises from $\sim 69\%$ to $\sim 76\%$ at *base-case* and operating pressure of 4 bar. After this modification the Bi-SOC energy efficiency further improves from $\sim 49\%$ to $\sim 54\%$.

The year-round CE analysis is carried out for the Bi-SOC system, with fuel cell fed with syngas, at 4 bar with and without SOEC air recirculation. Fig. 11 illustrates the system exergy efficiency as a function of SOFC mode operational time, while Fig. 12 depicts the system exergy losses and the components exergy destruction in the case of air recirculation integrated in the SOEC system.

It can be observed that the outlet exergy losses decrease from 23% to 16% due to air recirculation during electrolysis mode and operation at reduced pressure. The stack exergy loss grows as its resistance is inversely proportional to the operating pressure. Table 16 offers the percentage exergy flow of all components as compared to the inlet exergy in the different system configurations analysed.

When operating at 4 bar with H_2 as fuel, in fuel cell at *improved-case* conditions (SOFC-GT system energy efficiency of $\sim 78\%$), and in electrolyser mode with air recirculation at *base-case* conditions (SOEC system energy efficiency of $\sim 76\%$), the Bi-SOC energy efficiency increases up to $\sim 66\%$. This efficiency might improve further depending on the source of the heat provided to the electrolyser and the utilisation of the upgraded fuel produced from the SOC system. For instance, efficiency improvement can be obtained by operating the SOEC closer to the thermoneutral region, by feeding the pressurized H_2 produced when storing electricity into the stack when working in power production mode, and by optimising the thermal management required to heat up or cool down the electrolyser.

5. Conclusion and perspective

This work aims to assessing the thermodynamic feasibility of Bi-SOC systems and presents a refined view point on their design and operation. Moreover, this work intends to introduce a new method for analysing Bi-SOC system performance and optimising its design. The method is capable of taking into account the efficiencies in each system operating based on the energy demand and production curves.

We have carried out thermodynamic analyses of a Bi-SOC system with different plant configurations. We have attempted to maximize energy and exergy efficiency by varying the system layout and by enhancing the performance of SOC stack and BoP components. The enhancement was done with an energy and exergy analysis of individual systems identifying the largest losses and thus the opportunities for improvement. Optimal SOC stack operating parameters were selected via a sensitivity analysis on temperature, pressure, fuel utilisation, and fuel composition.

SOC stack operating conditions considerably affect the system performance. Systems can achieve high efficiencies at higher temperature and fuel utilisation. Moreover, in several configurations, the SOC stack together with the heat exchangers are the main cause of exergy destruction. The exergy losses in the exhaust stream is the highest contributor to reduction in the exergy efficiency. Integration of the gas turbine and air recirculation in the fuel cell system enhances its energy and exergy efficiencies, boosting the use of hot product gas for additional preheating treatment, and lowering the rate of exergy destruction.

Variation of operating conditions, configurations and SOC stack parameters showed a variation of Bi-SOC energy efficiency from 29% to 49% when the operating conditions are maintained equal in the two modes. The year-round cumulative exergy efficiency varies from 33% to 73% due to the selection of working parameters and the variation in operational time of the system in both modes. Optimising the stack parameters to suit both operating modes is crucial to achieve high year-round CE efficiencies. The SOEC efficiency increases with increasing current density whereas the SOFC performance increases with decreasing current density. Thus, considering the SOC to function in both modes at different current densities, Bi-SOC system energy efficiency at 4 bar increases from 49% to 54%. The incorporation of air recirculation also in the electrolysis mode and operating the system at 4 bar lead to a system energy efficiency of around 66% and a decrease of the exhaust exergy losses to 15%.

The year round cumulative exergy analysis is an annual operational time-weighted average of the SOFC and SOEC performances that takes into account the operating mode of the system based on the daily and seasonal variation of renewable energy production. The analysis carried on with this method introduced points to the need for careful system configuration and operating parameters adoption taking into account the number of operating hours per year, in either modes in order to achieve high efficiencies. This approach can be implemented when numerous small systems are used in parallel to meet the changing loads. A selected number of the systems can then be switched on or off but always the operating ones will be at design points. Moreover, the CE method with further improvements might also be helpful for analysing the system in case of off-design conditions. It may also help with estimating the system sizing and in selecting appropriate operating parameters based on the power production and consumption curve for a year.

Exergy and energy efficiencies might be increased by further optimising the system, such as by working in electrolyser mode close to thermoneutral region, by introducing a recirculation loop between anode and cathode, by improving the heat utilisation via proper thermal management (exchanging heat between the flows in both operation modes, so that the generated heat in fuel cell mode is exploited to enable the stack endothermic operation in electrolysis mode). These

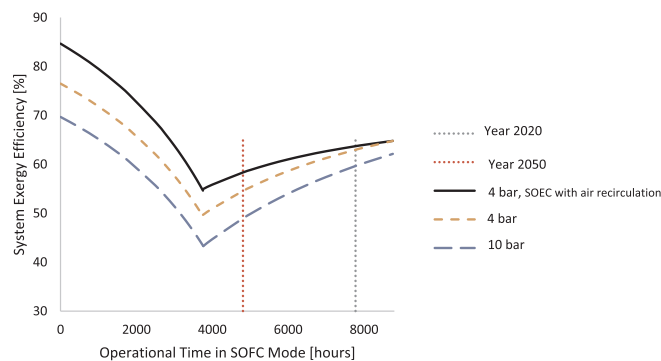


Fig. 11. Variation of the Bi-SOC system year-round exergy efficiency with the operational hours of the system in SOFC mode. Syngas is used as a fuel in the *base-case*, at 10 bar and 4 bar with and without SOEC air recirculation.

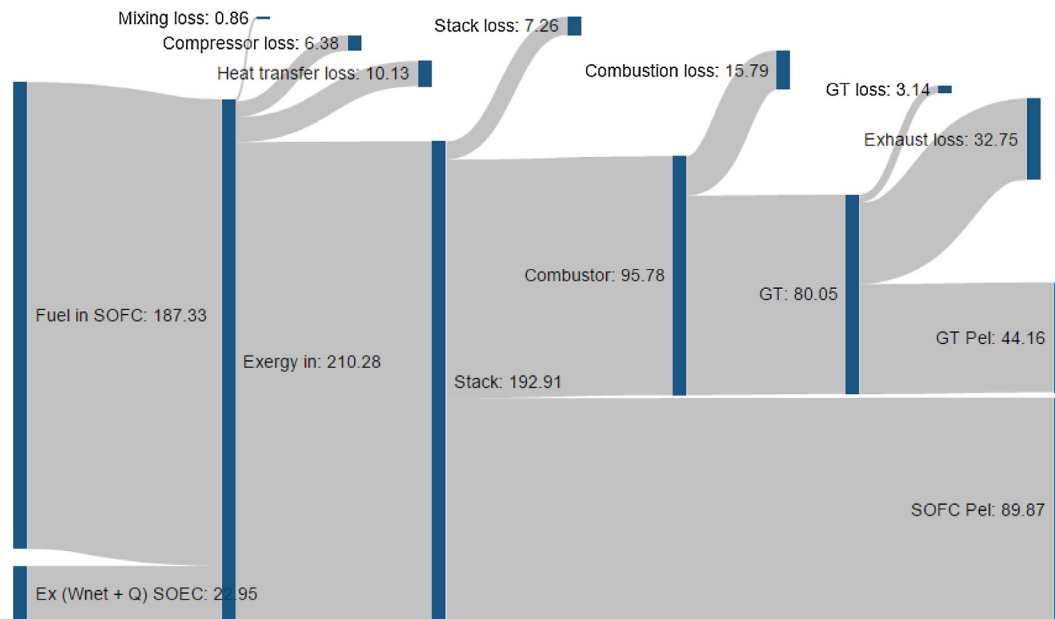


Fig. 12. Exergy flow diagram for the *base-case* Bi-SOC system at 4 bar, when the fuel cell is fed with syngas and the SOEC is running with air recirculation, during the year 2020. All values are in GWh.

Table 16

Exergy flow fraction of all components compared to the system inlet exergy for Bi-SOC system, with syngas as inlet fuel with pressure of 10 bar and 4 bar (with and without air recirculation), in year 2020.

	Component	10 bar	4 bar	4bar with SOEC air recirculation
		Fraction [%]	Fraction [%]	Fraction [%]
	Inlet Exergy	100	100	100
DESTRUCTION	Mixing	0.71	0.41	0.41
	Heat Transfer	2.96	4.84	4.82
	Compressor	3.26	3.15	3.03
	Stack	2.75	3.41	3.45
	Combustor	6.60	7.42	7.51
	GT	1.71	1.48	1.49
	Net destruction	17.99	20.70	20.71
	Exhaust losses	22.53	16.36	15.57
	GT P _{EL}	15.40	20.75	21.00
	SOFC P _{NET}	44.26	42.23	42.74
	Net Useful Exergy Out	-60	-63	-64

optimisation efforts are planned as our future work. The system exergy destruction might be further decreased by reducing present day resistance of the cell. Moreover, considering the increasing share of renewable energies in the global electricity production, in the future, the SOC stack is expected to operate more hours in SOEC mode. As a result, the overall system efficiency might increase even further.

This study provides useful insights on Bi-SOC systems and on the methodology that can be used for the initial design and evaluation of optimum system configuration and operating parameters. The CE method introduced in this manuscript, for the first time in the SOCs context, has not been used yet for analysing Bi-SOC systems. Conversely, round trip efficiency has been most often used. Results presented in this paper suggest that year round cumulative exergy efficiencies provide a better indicator for the selection of stack operating parameters and system configuration since it takes into account how much time a system works in each mode. Therefore, we hope the CE method will be used next to or instead of round trip efficiency analysis by a larger number of system developers and members of the SOC community.

Nevertheless, further research is beneficial in refining the concepts

presented in this manuscript and using the results thus obtained in identifying appropriate system design and operation choices in order to achieve high efficiencies for Bi-SOC systems in anticipated future energy systems, grids, and scenarios. Of particular interest will be the decisions on system scales, operation at or away from thermo-neutral points, operation at design or off-design conditions, as well as managing the system transients and the thermal discrepancy between fuel cell (exothermic) and electrolysis (typically endothermic or near thermo-neutral), all keeping an eye on achievable efficiencies. Ongoing and future activities in our group centre around the challenges mentioned above.

Acknowledgements

The authors wish to thank Theo Woudstra from TU Delft for the helpful discussions on the thermodynamic aspects of the study and the Energy Delta Gas Research (EDGaR) program that funded this research.

References

- [1] IPCC. Summary for policymakers, climate change 2014: mitigation of climate change. Contribution of working Group III to the fifth assessment report of the intergovernmental panel on climate change. In: Change UIPOC, editor. Cambridge; 2014.
- [2] Weyant JP, Blanford JG, Volker K, Clarke L, Edmonds J, Fawcett A, et al. The role of technology for achieving climate policy objectives: overview of the EMF 27 study on global technology and climate policy strategies. *Clim Change* 2014;123:353–67.
- [3] IEA. Energy Technology Perspectives 2015 - Mobilising Innovation to Accelerate Climate Action. Paris, France: International Energy Agency; 2015.
- [4] Denholm P, Ela E, Kirby B, Milligan M. The role of energy storage with renewable electricity generation. National Renewable Energy Laboratory; 2010.
- [5] Bruce D, Haresh K, Jean-Marie T. Electrical energy storage for the grid: a battery of choices. *Science* 334:928–35.
- [6] Hemmes K, Guerrero JM, Zhelev T. Highly efficient distributed generation and high-capacity energy storage. *Chem Eng Process Process Intensif* 2012;51:18–31.
- [7] Dell RM, Rand DAJ. Energy storage—a key technology for global energy sustainability. *Power Source* 2001;100:2–17.
- [8] Lindley D. Smart grids: the energy storage problem. *Nature* 2010;463:18–20.
- [9] Graves C, Ebbesen SD, Mogensen M, Lackner KS. Sustainable hydrocarbon fuels by recycling CO₂ and H₂O with renewable or nuclear energy. *Renew Sustain Energy Rev* 2011;15:1–23.
- [10] Minh NQ, Mogensen MB. Reversible solid oxide fuel cell technology for green fuel and power production. *The Electrochemical Society Interface*; 2013.
- [11] Graves C, Ebbesen S, Jensen S, Simonsen S, Mogensen M. Eliminating degradation in solid oxide electrochemical cells by reversible operation. *Nat Mater* 2015;14:239–44.
- [12] Al-musleh EI, Mallapragada DS, Agrawal R. Continuous power supply from a baseload renewable power plant. *Appl Energy* 2014;122:83–93.
- [13] Jensen SH, Graves C, Mogensen M, Wendel C, Braun R, Hughes G, et al. Large-scale electricity storage utilizing reversible solid oxide cells combined with underground storage of CO₂ and CH₄. *Energy Environ Sci* 2015;8:2471–9.
- [14] Ohmori H, Iwai H, Itakura K, Saito M, Yoshida H. Numerical prediction of system round-trip efficiency and feasible operating conditions of small-scale solid oxide iron–air battery. *Power Sources* 2016;309:160–8.
- [15] Braun RJ. Techno-economic optimal design of solid oxide fuel cell systems for micro-combined heat and power applications in the U.S. *J Fuel Cell Sci Technol* 2010;7:031018.
- [16] Whiston MM, Collinge WO, Bilec MM, Schaefer LA. Exergy and economic comparison between kW-scale hybrid and stand-alone solid oxide fuel cell systems. *J Power Sources* 2017;353:152–66.
- [17] Khani L, Mahmoudi SMS, Chitsaz A, Rosen MA. Energy and exergoeconomic evaluation of a new power/cooling cogeneration system based on a solid oxide fuel cell. *Energy* 2016;94:64–7.
- [18] Bang-Møller C, Rokni M, Elmegaard B. Exergy analysis and optimization of a biomass gasification, solid oxide fuel cell and micro gas turbine hybrid system. *Energy* 2011;36:4740–52.
- [19] Hajabdollahi Z, Fu P-F. Multi-objective based configuration optimization of SOFC-GT cogeneration plant. *Appl Therm Eng* 2017;112:549–59.
- [20] Hosseinpour J, Sadeghi M, Chitsaz A, Ranjbar F, Rosen MA. Exergy assessment and optimization of a cogeneration system based on a solid oxide fuel cell integrated with a Stirling engine. *Energy Convers Manage* 2017;143:448–58.
- [21] Wang M, Wang Z, Gong X, Guo Z. The intensification technologies to water electrolysis for hydrogen production: a review. *Renew Sustain Energy Rev* 2014;29:573–88.
- [22] Laguna-Becero MA. Recent advantages in high temperature electrolysis using solid oxide fuel cells: a review. *J Power Sources* 2012;203:4–16.
- [23] Zheng Y, et al. A review of high temperature co-electrolysis of H₂O and CO₂ to produce sustainable fuels using solid oxide electrolysis cells (SOECs): advanced materials and technology. *Chem Soc Rev* 2017;46.
- [24] Redissi Y, Bouallaou C. Valorization of carbon dioxide by Co-electrolysis of CO₂/H₂O at high temperature for syngas production. *Energy Proc* 2013;37:202–13.
- [25] De Saint Jean M, Baurens P, Bouallou C, Couturier K. Economic assessment of a power-to-substitute-natural-gas process including high-temperature steam electrolysis. *J Hydrogen Energy* 2015;40:6487–500.
- [26] Varone A, Ferrari M. Power to liquid and power to gas: an option for the German Energiewende. *Renew Sustain Energy Rev* 2015;45:207–18.
- [27] Guendalini G, Campanari S, Romano MC. Power-to-gas plants and gas turbines for improved wind energy dispatchability: energy and economic assessment. *Appl Energy* 2015;147:117–30.
- [28] I-o Karitha, et al. Flowsheet-based model and exergy analysis of solid oxide electrolysis cells for clean hydrogen production. *J Clean Prod* 2018;170:1–13.
- [29] Union PootE. Programme review report 2014 - Fuel cell and Hydrogen joint undertaking; 2015.
- [30] Von Olshausen C. Project status - liquid hydrocarbon from CO₂ and H₂O and renewable electricity. BMBF Statusseminar. Berlin, Germany: Sunfire; 2015.
- [31] Walter C. SOEC development status at sunfire GmbH. Technical Forum presentation. HANNOVER MESSE; 2014.
- [32] Krause M-SG. Inventurliste der relevanten Forschungs- und DemoProjekte im Rahmen der Roadmap-Erstellung. Freiberg: Gastechnologisches Institut GmbH; 2014.
- [33] Gruber M, Harth S, Trimis D, Bajohr S, Posdziech O, Brabandt J, et al. Integrated high-temperature electrolysis and methanation for effective Power to Gas conversion (HELMETH). Gasfachliche Aussprachetagung. Essen, Germany: Karlsruhe Institut für Technologie; 2015.
- [34] Hansen JB, Petersen AS, Loncarevic I, Torbensen C, Korsgaard A, Christensen SL. GreenSynFuels - Final project Report. Danish Technological Institute; 2011.
- [35] Biogas-SOEC Electrochemical upgrading of biogas to pipeline quality by means of SOEC electrolysis, 2012. Main Final Report ForskNG 2011, Project no 10677, Haldor Topsoe.
- [36] www.ae-energianalyse.dk. Electrolysis by means of SOEC. Project Information; 2015 [accessed 10.09.15].
- [37] Sustainable synthetic fuels from biomass gasification and electrolysis, SYNFUEL, Project Information; 2015 [accessed 10.09.15].
- [38] Moritz H, Willich C, Kallo J, Friedrich AK. Theoretical study on pressurized operation of solid oxide electrolysis cells. *Int J Hydrogen Energy* 2014;39.
- [39] Strohbach T, Mittmann F, Walter C, Schmanke D. Sunfire Industrial SOC Stacks and Modules. *ECS Trans* 2015;68:125–9.
- [40] Perna A, Minutillo M, Cicconardi SP, Jannelli E, Scarfogliero S. Performance assessment of electric energy storage (EES) systems based on reversible solid oxide cell. *Energy Proc* 2016;101:1087–94.
- [41] Wendel CH, Kazempour P, Braun RJ. A thermodynamic approach for selecting operating conditions in the design of reversible solid oxide cell energy systems. *J Power Sources* 2015;301.
- [42] Kazempour P, Braun RJ. Model validation and performance analysis of regenerative solid oxide cells for energy storage applications: reversible operation. *Int J Hydrogen Energy* 2015;39.
- [43] Hauck M, Herrmann S, Spliethoff H. Simulation of a reversible SOFC with Aspen Plus. *Int J Hydrogen Energy* 2017;42.
- [44] Mottaghizadeh P, et al. Process modeling of a reversible solid oxide cell (r-SOC) energy storage system utilizing commercially available SOC reactor; 2017;142.
- [45] Bronchart F, Paepe MD, Dewulf J, Schrevels E, Demeyer P. Thermodynamics of greenhouse systems for the northern latitudes: Analysis, evaluation and prospects for primary energy saving. *J Environ Manage* 2013;119:121–33.
- [46] Zhang Z, Pan Y, Huang H, Jiang Q. Performance experiment of all fresh air-handling unit with high sub-cooling degree and year-round exergy analysis. *HVAC&R Res* 2014;20:810–8.
- [47] Botta G, Solimeo M, Leone P, Aravind PV. Thermodynamic analysis of coupling a SOEC in co-electrolysis mode with the dimethyl ether synthesis. *Fuel Cell* 2015;15:669–81.
- [48] Botta G, Patel HC, Sebastiani F, Aravind PV. Thermodynamic and exergy analysis of reversible solid oxide cell systems. In: ECS Conference on Electrochemical Energy Conversion & Storage, SOFC-XIV, Glasgow; 2015.
- [49] Jensen S, Sun X, Ebbesen S, Knibbe R, Mogensen M. Hydrogen and synthetic fuel production using pressurized solid oxide electrolysis cells. *Int J Hydrogen Energy* 2010;35:9544–9.
- [50] Ebbesen SD, Graves C, Mogensen M. Production of synthetic Fuels by Co-Electrolysis of Steam and Carbon Dioxide. *Int J Green Energy* 2009;6.
- [51] Gandiglio M, Lanzini A, Leone P, Santarelli M, Borchelli R. Thermoeconomic analysis of large solid oxide fuel cell plants: Atmospheric vs. pressurized performance. *Energy* 2013:142–55.
- [52] Graves C, Ebbesen SD, Mogensen M, Lackner KS. Sustainable hydrocarbon fuels by recycling CO₂ and H₂O with renewable or nuclear energy. *Renew Sustain Energy Rev* 2011;1–23.
- [53] Groot AD. Advanced exergy analysis of high temperature fuel cell systems, available at uid:f1489e9e-d50b-49f9-8e66-3c35c03eae3b [Dissertation]: The Energy research Centre of the Netherlands (ECN); 2004.
- [54] Sun X, Chen M, Jensen SH, Ebbesen SD, Graves C, Mogensen M. Thermodynamic analysis of synthetic hydrocarbon fuel production in pressurized solid oxide electrolysis cells. *Int J Hydrogen Energy* 2012;37:17101–10.
- [55] Giglio E, Lanzini A, Santarelli M, Leone P. Synthetic natural gas via integrated high-temperature electrolysis and methanation: part I - energy performance. *J Storage Mater* 2015;1:22–37.
- [56] Penchini D, Cinti G, Disceppli G, Desideri U. Theoretical study and performance evaluation of hydrogen production by 200 W solid oxide electrolyser stack. *Hydrogen Energy* 2014;39:9457–66.
- [57] Ferrero D, Lanzini A, Leone P, Santarelli M. Reversible operation of solid oxide cells under electrolysis and fuel cell modes: experimental study and model validation. *Chem Eng J* 2015;274:143–55.
- [58] Fu Q, Mabilat C, Zahid M, Brisse A, Gautier L. *Energy Environ Sci*. 2010;3.
- [59] Obrien JE. *J Heat Transf* 2012;134.
- [60] Aguiar P, Brandon NP, Udagawa J. Hydrogen production through steam electrolysis: Model-based dynamic behaviour of a cathode-supported intermediate temperature solid oxide electrolysis cell. *J Power Sources* 2008;180:46–88.
- [61] Tabish AN, Patel HC, Aravind PV. Electrochemical oxidation of syngas on nickel and ceria anodes. *Electrochim Acta* 2017;228:575–85.
- [62] El-Sayed AF. *Aircraft Propulsion and Gas Turbine Engines*; 2008.
- [63] Lora P, Taher MAA, Chiesa P, Brandon NP. A novel system for the production of pure hydrogen from natural gas based on solid oxide fuel cell–solid oxide electrolyzer. *Int J Hydrogen Energy* 2010;35:12680–7.
- [64] Woudstra N. Sustainable energy systems [Dissertation]. Delft: TU Delft; 2012.
- [65] Moran J, Shapiro H. Fundamentals of engineering thermodynamics, 7th ed. John Wiley & Sons, Inc.; 2006.
- [66] Deuchler R. Load management-strategies for dealing with temporary oversupply of variable renewable electricity. Utrecht University 2013.
- [67] Franka M, Dejar R, Petersa R, Bluma L, Stoltena D. Bypassing renewable variability with a reversible solid oxide cell plant. *Appl Energy* 2018;217.
- [68] Doherty W, Reynolds A, Kennedy D. Aspen plus Simulation of biomass gasification in a steam blown dual fluidized bed; 2013.
- [69] Fernandes A, Woudstra T, Aravind PV. System simulation and exergy analysis on

- the use of biomass-derived liquid-hydrogen for SOFC/GT powered aircraft. *Int J Hydrogen Energy* 2015;40.
- [70] Tao G, Butler B, Virkar AV. Hydrogen and power by fuel-assisted electrolysis using solid oxide fuel cells; 2011.
- [71] Botta G, Solimeo M, Leone P, Aravind PV. synthetic natural gas production via co-electrolysis. In: 11th european sofc&soec forum. Lucerne; 2014.
- [72] Brisse A, Schefold J, Zahid M. High temperature water electrolysis in solid oxide cells. *Int J Hydrogen Energy* 2008;33:5375–82.
- [73] Cinti G, Baldinelli A, Michele AD, Desideri U. Integration of solid oxide electrolyzer and Fischer-Tropsch: a sustainable pathway for synthetic fuel. *Appl Energy* 2016;162:308–20.
- [74] Milewski J, Swirski K, Santarelli M, Leone P. Advanced methods of solid oxide fuel cell modeling: Springer; 2011.
- [75] Aravind PV, Schilt C, Turker B, Woudstra T. *Int J Renew Energy Dev*; 2012.
- [76] O'Brien JE, McKellar MG, Stoots CM, Herring JS, Hawkes GL. *International J. Hydrogen Energy*; 2009.
- [77] Barelli L, Bidini G, Ottaviano A. Part load operation of SOFC-GT hybrid systems: stationary. *Int J Hydrogen Energy* 2012;37:16140–50.
- [78] Patel HC, Woudstra T, Aravind PV. Thermodynamic analysis of solid oxide fuel cell gas turbine systems operating with various biofuels. *Fuel Cells* 2012;12:1115–28.
- [79] Cai Q, Brandon NP, Adjiman CS. Modelling the dynamic response of a solid oxide steam electrolyser to transient inputs during renewable hydrogen production. *Front Energy Power Eng China* 2010;4:211–22.
- [80] Mitsubishi Heavy Industries Ltd. Gas turbine combined cycle (GTCC) & integrated coal gasification combined cycle (IGCC); 2018.
- [81] Jörg A, Balzer CH, Louis J, Schabla U. SHELL HYDROGEN STUDY ENERGY OF THE FUTURE? Sustainable mobility through fuel cells and H₂. 22284 Hamburg: Published by Shell Deutschland Oil GmbH; 2017.
- [82] Options for producing low-carbon hydrogen at scale. Policy briefing: The Royal Society; 2018.
- [83] European Commission's Directorates-General for Energy Research & Innovation and Joint Research Centre. Integrated Strategic Energy Technology (SET) Plan Progress in 2016. Luxembourg: Publications Office of the European Union; 2016.